Inorganic Chemistry

Article

pubs.acs.org/IC

Counteranion and Solvent Assistance in Ruthenium-Mediated Alkyne to Vinylidene Isomerizations

Manuel Jiménez-Tenorio,* M. Carmen Puerta,* and Pedro Valerga

Departamento de Ciencia de los Materiales e Ingeniería Metalúrgica y Química Inorgánica, Facultad de Ciencias, Universidad de Cádiz, 11510 Puerto Real, Cádiz, Spain

Manuel A. Ortuño, Gregori Ujaque, and Agustí Lledós*

Departament de Química, Universitat Autònoma de Barcelona, 08193 Cerdanyola del Vallès, Barcelona, Spain

Supporting Information

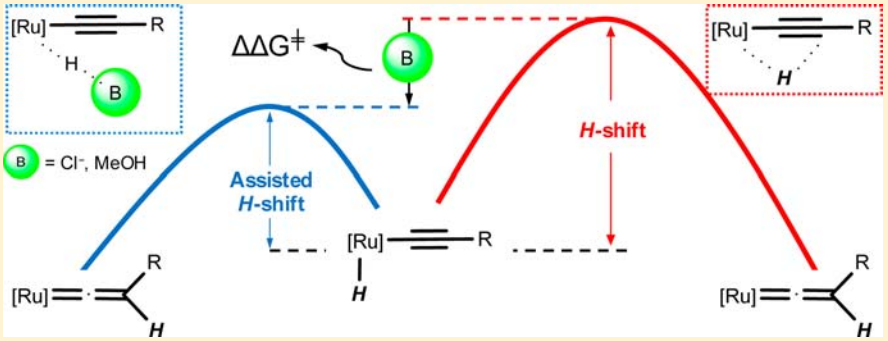

ABSTRACT: The complex [Cp*RuCl(^{i}Pr$_2$PNHPy)] (**1**) reacts with 1-alkynes HC≡CR (R = COOMe, $C_6H_4CF_3$) in dichloromethane furnishing the corresponding vinylidene complexes [Cp*Ru=C=CHR(^{i}Pr$_2$PNHPy)]Cl (R = COOMe (**2a-Cl**), $C_6H_4CF_3$ (**2b-Cl**)), whereas reaction of **1** with $NaBPh_4$ in MeOH followed by addition of HC≡CR (R = COOMe, $C_6H_4CF_3$) yields the metastable π-alkyne complexes [Cp*Ru(η^2-HC≡CR)(^{i}Pr$_2$PNHPy)][BPh_4] (R = COOMe (**3a-BPh$_4$**), $C_6H_4CF_3$ (**3b-BPh$_4$**)). The transformation of **3a-BPh$_4$**/**3b-BPh$_4$** into their respective vinylidene isomers in dichloromethane is very slow and requires hours to its completion. However, this process is accelerated by addition of LiCl in methanol solution. Reaction of **1** with HC≡CR (R = COOMe, $C_6H_4CF_3$) in MeOH goes through the intermediacy of the π-alkyne complexes [Cp*Ru(η^2-HC≡CR)(^{i}Pr$_2$PNHPy)]Cl (R = COOMe (**3a-Cl**), $C_6H_4CF_3$ (**3b-Cl**)), which rearrange to vinylidenes in minutes, i.e., much faster than their counterparts containing the $[BPh_4]^-$ anion. The kinetics of these isomerizations has been studied in solution by NMR. With the help of DFT studies, these observations have been interpreted in terms of chloride- and methanol-assisted hydrogen migrations. Calculations suggest participation of a hydrido−alkynyl intermediate in the process, in which the hydrogen atom can be transferred from the metal to the β-carbon by means of species with weak basic character acting as proton shuttles.

INTRODUCTION

Transition-metal-mediated alkyne to vinylidene isomerization is a well-known process which has attracted much attention from both experimental and theoretical points of view,[1−17] with particular emphasis on its relevance to the catalytic transformations of alkynes.[18−21] Detailed theoretical studies supported by experimental work have been performed on several systems.[5−11,13,15−17] Among those, systems containing ruthenium can be considered particularly remarkable.[2,3,6,7c,9,10] Two mechanisms have been proposed to explain the alkyne to vinylidene isomerization process (Scheme 1): direct intramolecular 1,2-hydrogen shift in a π-alkyne complex (route **A**), or 1,3-hydrogen shift from a hydrido−alkynyl complex (route **B**), formed by oxidative addition of the 1-alkyne to the unsaturated metal center.

Variants of the two pathways shown before have been described in detail. The 1,2-H shift may occur through the intermediacy of a CH σ-bonded complex of the type [M(η^2-H−C≡CR)L_n][8−10,14] (route **AI**) or alternatively through formation of a η^2-vinylidene complex [M(η^2-C=CHR)L_n] (route **AII**). Theoretical studies suggest that the pathway involving the η^2-H−C≡CR complex is lower in energy (**AI**) and hence more feasible.[8−10,14] From the η^2-H−C≡CR intermediate, it is possible to access the hydrido−alkynyl complex [MH(C≡CR)L_n] in a straightforward manner. Ulterior 1,3-H shift leads to the final vinylidene product (route **B**).

Received: May 5, 2013
Published: July 8, 2013

   dx.doi.org/10.1021/ic401119p | *Inorg. Chem.* 2013, 52, 8919−8932

Scheme 1. Proposed Mechanisms for Transition-Metal-Mediated Alkyne to Vinylidene Isomerization

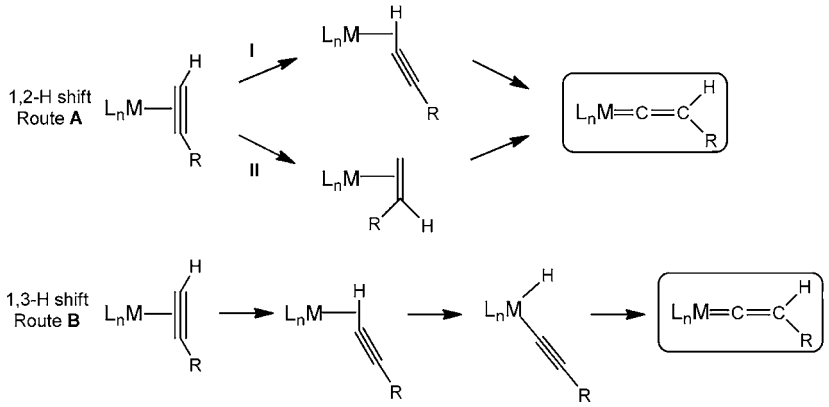

The direct 1,2-H shift appears to be the most widespread mechanism for the alkyne to vinylidene rearrangement. A formally analogous mechanism has been proposed and theoretically modeled for the Ru-mediated isomerization of internal alkynes to yield disubstituted vinylidene complexes.[22] In these cases, one of the alkyne substituents of the alkyne moiety migrates from one carbon atom to the other. The process has been also observed to occur in the solid state. At variance with this, direct 1,3-H shift from a hydrido−alkynyl species is more elusive and still a matter of debate. Calculations from Wakatsuki et al. for isomerization of the model ruthenium complex $[RuCl_2(\eta^2\text{-}HC{\equiv}CH)(PH_3)_2]$ to $[Ru{=}C{=}CH_2(Cl)_2(PH_3)_2]$ showed that the intermediate $[RuCl_2(H)(C{\equiv}CH)(PH_3)_2]$ was of very high energy and, therefore, highly unstable.[7c] In the system $[CpRuH(C{\equiv}CH)(PMe_3)_2]^+$, the intramolecular 1,3-hydrogen shift can be ruled out due to its high energy barrier.[9,10] However, the oxidative addition reaction has a relatively low barrier and might in fact become a competitive process with the π coordination of the alkyne on this electron-rich fragment.[10] It appears that the mechanism involving oxidative addition is difficult if the metal changes from d^6 to d^4, as in the case of Ru^{II} to Ru^{IV}, but becomes feasible in the case of highly electron-rich d^6 metal fragments and also in those instances in which the metal changes from d^8 to d^6, i.e., M^I to M^{III} (M = Co, Rh, Ir).[1,11−17] Despite the fact that calculations rule out hydrido−alkynyl to vinylidene rearrangements through intramolecular 1,3-hydrogen shift, we have shown that the isolable hydrido−alkynyl complexes $[Cp^*RuH(C{\equiv}CR)(dippe)]^+$ (dippe = bis(1,2-diisopropylphosphino)ethane)[3] as well as $[Cp^*RuH(C{\equiv}CR)(P)_2]^+$ (P = PMe^iPr_2, PEt_3)[6,23] undergo isomerization to the respective vinylidene derivatives. The proposed mechanism involves deprotonation of the hydride to yield a neutral σ-alkynyl complex followed by protonation at the β-carbon.

A similar mechanism, involving a base-assisted proton migration from an intermediate ethynyl−vinylidene, has been invoked in the case of the butadiyne to butatrienylidene isomerization in $[CpRu(HC{\equiv}CC{\equiv}CH)(PMe_3)_2]^+$, which has been modeled by DFT calculations.[24] In the case of d^8 metal complexes, a bimolecular mechanism has been proposed for the alkyne to vinylidene isomerization on the fragment $\{RhCl(P^iPr_3)_2\}$ via formation of the dimeric d^6 hydrido−alkynyl intermediate $[\{RhHCl(C{\equiv}CR)(P^iPr_3)_2\}_2]$.[1b,11] However, other researchers have gathered theoretical and experimental evidence in support of an alternative mechanism for this process which does not involve dimeric species.[13,14,17] Thus, double-crossover experiments using the deuterium- and ^{13}C-labeled compound $[RhCl(\eta^2\text{-}D^{13}C{\equiv}^{13}CD)(P^iPr_3)_2]$ together with the nonlabeled derivative $[RhCl(\eta^2\text{-}HC{\equiv}CH)(P^iPr_3)_2]$ were carried out. These experiments led to the respective vinylidene complexes $[Rh{=}^{13}C{=}^{13}CD_2(Cl)(P^iPr_3)_2]$ and $[Rh{=}C{=}CH_2(Cl)(P^iPr_3)_2]$, and no H/D scrambling was observed. This result is inconsistent with the significant involvement of a bimolecular mechanism, and hence, a direct 1,3-H shift is considered to be the preferred reaction pathway. Interestingly, for these rhodium-based systems it has been observed that the presence of a basic imidazol-2-yl substituent on the phosphine used as coligand causes a dramatic increase in the rate of the alkyne to vinylidene isomerization, i.e., when mediated by $[RhCl(P^iPr_2Im)_2]$ (Im = 1-methyl-4-*tert*-butylimidazol-2-yl) instead of $[\{RhCl(P^iPr_2Ph)_2\}_2]$.[13,14] Werner and coworkers already observed an acceleration of the transformation of $[RhCl(HC{\equiv}CR)(P^iPr_3)_2]$ into $[Rh{=}C{=}CHR(Cl)(P^iPr_3)_2]$ upon addition of pyridine to the reaction mixture.[1] These observations have been interpreted in terms of the electron-donating abilities of the basic heterocyclic phosphine substituents as well as their steric properties.[14]

In recent years, an increasing amount of evidence has revealed the influence that ion pairing can have in organometallic transformations,[25] particularly in those involving proton transfer steps. Ion-pairing formation can modify the energy barrier of a proton transfer reaction by stabilization or destabilization of reaction intermediates, as shown in the kinetic study of the deprotonation of the cationic dihydrogen complex *trans*-$[FeH(\eta^2\text{-}H_2)(dppe)_2]^+$ with NEt_3.[26] Counterions can also influence the rate of a reaction by opening up new reaction pathways of lower energy, as found in the theoretical study of the gold(I)-catalyzed hydroamination of 1,3-dienes.[27] Proton transfer can also be favored by stabilizing the transition state through creation of an efficient network of H bonds between the anion and the migrating proton.[28]

Fostered by these previous observations, we wondered whether alkyne → vinylidene isomerizations, which involve a proton migration step, could be affected by anions. To our delight, we observed that addition of LiCl (in methanol) to dichloromethane solutions of the metastable π-alkyne complexes $[Cp^*Ru(\eta^2\text{-}HC{\equiv}CR)(^iPr_2PNHPy)][BPh_4]$ (R = COOMe, $C_6H_4CF_3$) causes an acceleration in the rate of isomerization to the corresponding vinylidene complexes $[Cp^*Ru{=}C{=}CHR)(^iPr_2PNHPy)][BPh_4]$ (R = COOMe, $C_6H_4CF_3$). In the absence of chloride ion, the isomerization process is very slow and takes hours to occur completely. At

dx.doi.org/10.1021/ic401119p | *Inorg. Chem.* 2013, 52, 8919−8932

variance with this, direct reaction of the chlorocomplex [Cp*RuCl(^{i}Pr$_2$PNHPy)][29] with HC≡CR (R = COOMe, $C_6H_4CF_3$) in MeOH leads to the vinylidene complexes [Cp*Ru=C=CHR(^{i}Pr$_2$PNHPy)][Cl] in minutes. Addition of MeOH to [Cp*Ru(η^2-HC≡CR)(^{i}Pr$_2$PNHPy)][BPh_4] (R = COOMe, $C_6H_4CF_3$) in dichloromethane solution also causes an acceleration in the rate of isomerization. This suggests that certain solvents may also play a significant role in this process. In order to clarify the influence of the chloride ion and MeOH in the alkyne to vinylidene isomerization process, DFT calculations were carried out for the HC≡CCOOMe alkyne in methanol solvent. By means of computational methods, formation of hydrogen bonding between chloride and the NH spacer group of the hemilabile phosphine has been revealed[20,30] and the role of the chloride ion and MeOH in the isomerization process has been analyzed. We found that a base-assisted proton transfer through a hydrido−alkynyl intermediate has a lower energy barrier than the direct hydrogen shift. Experimental and theoretical details are presented and discussed in this work.

RESULTS AND DISCUSSION

Experimental Study. The complex [Cp*RuCl(^{i}Pr$_2$PNHPy)] (**1**)[29] reacts with 1-alkynes HC≡CR (R = COOMe, $C_6H_4CF_3$) in dichloromethane at room temperature furnishing the corresponding vinylidene complexes [Cp*Ru=C=CHR(^{i}Pr$_2$PNHPy)]Cl (R = COOMe (**2a-Cl**), $C_6H_4CF_3$ (**2b-Cl**)). Treatment of solutions of these complexes in methanol with an excess of solid $NaBPh_4$ leads to metathetical counterion exchange, yielding the cationic vinylidene complexes in the form of $[BPh_4]^-$ salts, [Cp*Ru=C=CHR(^{i}Pr$_2$PNHPy)][BPh_4] (R = COOMe (**2a-BPh$_4$**(, $C_6H_4CF_3$ (**2b-BPh$_4$**)). NMR spectra of the chloride and tetraphenylborate salts, **2a-Cl**/**2a-BPh$_4$** and **2b-Cl**/**2b-BPh$_4$**, are very similar and fully consistent with the presence of vinylidene ligands in these complexes. The metal-bound carbon atom of the vinylidene appears as one characteristic low-field resonance around 340 ppm in the $^{13}C\{^1H\}$ NMR spectra in all cases. However, there are big differences in the observed chemical shifts of the NH proton resonance depending on the counterion present, either chloride or tetraphenylborate. Thus, the NH protons for the chloride salts **2a-Cl** and **2b-Cl** appear in the ^1H NMR spectra as broad singlets at 10.8 ppm, whereas the resonances for **2a-BPh$_4$** and **2b-BPh$_4$** are observed as doublets at 5.77 and 5.24 ppm, respectively. This indicates that the chemical shift of the NH proton is strongly influenced by the presence of the chloride ion. An observed difference of 5 ppm in the chemical shifts of the NH proton resonances when passing from **2a-Cl** to **2a-BPh$_4$** or from **2b-Cl** to **2b-BPh$_4$** cannot be ignored and must be accounted for. We attribute this large difference in chemical shifts to formation of a strong hydrogen bond between the NH proton and the chloride ion. It is known that hydrogen bonding causes a deshielding of protons, and a downfield shift for the corresponding proton resonances is anticipated. Strong deshielding has been recently observed for one of the NH proton resonances of 6-azauracile in the complex [Ru(η^3:η^3-$C_{10}H_{16}$)Cl_2L] (L = 6-azauracile).[31] A thorough NMR study carried out on this compound, including variable-temperature measurements and DOSY experiments, confirmed the existence of an intramolecular hydrogen bond between one NH and a Cl atom of the coordination sphere of the metal. In the case of **2a-Cl** and **2b-Cl**, the IR spectra do not show any unusual shifts in the positions of the ν(NH) bands, which appear in the range 3300−3400 cm^{-1}. We carried out ionic conductivity (Λ) measurements for complexes **2a/b-Cl** and **2a/b-BPh$_4$** in nitromethane solution (Table 1).

Table 1. Ionic Conductivity of 0.01 M Solutions of the Indicated Compounds in Nitromethane

compound	Λ (μS/cm)
2a-Cl	190
2a-BPh$_4$	440
2b-Cl	230
2b-BPh$_4$	439
[^{n}Bu$_4$N][BPh_4]	446

Ionic conductivities of **2a-Cl** and **2b-Cl** (0.01 M solution in nitromethane) are 190 and 230 μS/cm, respectively, whereas solutions of **2a-BPh$_4$** and **2b-BPh$_4$** of the same concentration have conductivities of ca. 440 μS/cm. The latter value is in the range expected for a 1:1 electrolyte, by comparison with the ionic conductivity measured for [^{n}Bu$_4$N][BPh_4] under the same conditions. These results indicate that the cationic complex and the chloride in **2a-Cl** and **2b-Cl** are strongly associated in solution in comparison with the situation of the anion and cation in the case of **2a-BPh$_4$** and **2b-BPh$_4$**. We can explain these data by considering a strong hydrogen bonding interaction between the chloride and the NH group of the ^{i}Pr$_2$PNHPy ligand, which leads to formation of a tight ion pair (Figure 1A). However, taking into account the potential

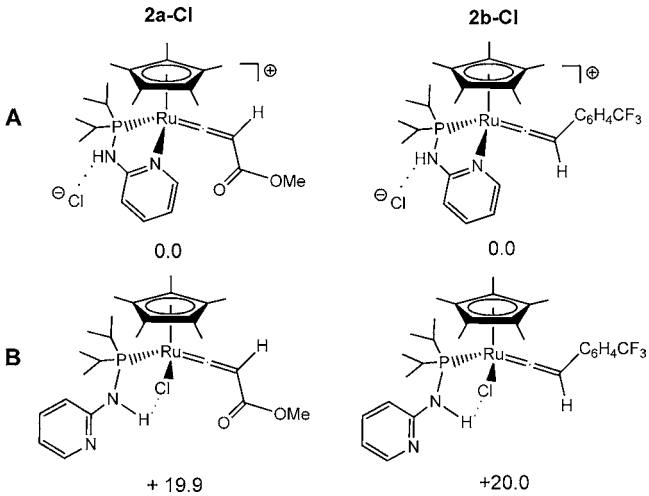

Figure 1. DFT-optimized geometries of alternative structures for compounds **2a-Cl** and **2b-Cl**. Relative Gibbs energies in methanol in kcal mol^{-1}.

hemilabile character of the ^{i}Pr$_2$PNHPy ligand,[29,32] we might also have a situation in which the chloride displaces the pyridyl group, furnishing a neutral chlorovinylidene complex bearing a monodentate κ^1-*P*-^{i}Pr$_2$PNHPy ligand, with an intramolecular hydrogen bonding interaction between the NH and the chloride (Figure 1B).

Our efforts to obtain single crystals of either **2a-Cl** or **2b-Cl** have been unsuccessful. This would have enabled us to determine unequivocally by means of X-ray crystallography which of the two possible situations depicted in Figure 1 is the actual one in the solid state. Therefore, we used DFT calculations for compounds **2a-Cl** and **2b-Cl** in order to compare the energies of the two possible structures. Optimized

dx.doi.org/10.1021/ic401119p | Inorg. Chem. 2013, 52, 8919−8932

geometries for both the A and the B forms of **2a-Cl** and **2b-Cl** can be found in the Supporting Information. Upon geometry optimization in methanol solution, the computational results clearly support ion pair formation in both complexes by ca. 20.0 kcal mol^{-1} (Figure 1). ^1H NMR calculations were also carried out on **2a-Cl** and **2b-Cl** as well as on the corresponding Cl-free **2a** and **2b**. As regards the N*H* proton, the calculated chemical shifts were 6.0 (**2a**) and 10.4 ppm (**2a-Cl**) for R = COOMe and 6.1 (**2b**) and 10.3 ppm (**2b-Cl**) for R = $C_6H_4CF_3$. The deshieldings of 4.4 (**2a**) and 4.2 ppm (**2b**) with respect to the Cl-free forms are in line with the value of 5 ppm experimentally observed. Hence, it is feasible to assume that in solution for both **2a-Cl** and **2b-Cl** we deal with cationic vinylidene complexes forming tight ion pairs with chloride.

Reaction of **1** with $NaBPh_4$ in MeOH followed by addition of HC≡CR (R = COOMe, $C_6H_4CF_3$) at 0 °C yields the π-alkyne complexes [Cp*Ru(η^2-HC≡CR)(^{i}Pr$_2$PNHPy)][BPh_4] (R = COOMe (**3a-BPh$_4$**), $C_6H_4CF_3$ (**3b-BPh$_4$**)). These compounds display one strong ν(C≡C) band at 1838 and 1816 cm^{-1}, respectively. NMR spectroscopy shows that these compounds consist of mixtures of two possible diastereomers present in a ratio close to 1:1. These two diastereomers result from two possible orientations of the π-alkyne ligand with respect to the phosphorus and pyridyl groups bound to ruthenium, as shown in Chart 1.

Chart 1

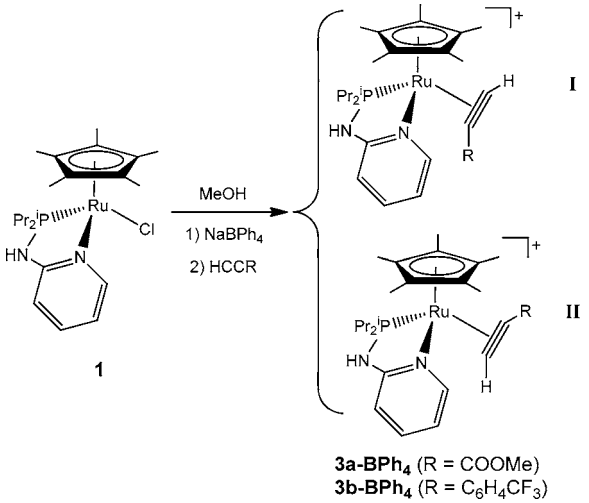

Each diastereomer shown gives rise to one broad resonance in the $^{31}P\{^1H\}$ NMR spectra, indicative of hindered rotation around the ruthenium–alkyne bond. These resonances get sharper when the temperature is lowered. For this reason, NMR spectra of these species were measured at 213 K. At this temperature, NMR spectra for **3a-BPh$_4$** and **3b-BPh$_4$** are well resolved and display two sets of resonances, one for each of the diastereomers shown in Chart 1. A similar behavior in solution has been observed for the related, recently reported π-alkyne complex [Cp*Ru(η^2-PhCOC≡CPh)(^{i}Pr$_2$PNHPy)][BPh_4], which has been structurally characterized.[22a]

If compound **1** is allowed to react with HC≡CR (R = COOMe, $C_6H_4CF_3$) in MeOH at room temperature and then treated with $NaBPh_4$ (that is, reversing the order in which the reagents are added with respect to the synthetic procedure outlined above for **3a-BPh$_4$** or **3b-BPh$_4$**), a yellow or pink precipitate is formed. Upon isolation by filtration, solids were identified by NMR spectroscopy as the vinylidene complexes **2a-BPh$_4$** or **2b-BPh$_4$**, containing some amount of π-alkyne complex **3a-BPh$_4$** or **3b-BPh$_4$** depending upon the reaction time and temperature. Whereas the amounts of **3b-BPh$_4$** present are usually very small, **3a-BPh$_4$** may represent up to 20% of the product in the mixture with **2a-BPh$_4$**. Clearly, the π-alkyne complexes are metastable species which undergo isomerization to vinylidene species, as observed in many other instances.[2−4,6] The fact that the product formed depends on the order in which the reagents are added to the metal complex has been previously observed by us in the case of the system [Cp*RuCl(dippe)] (dippe =1,2-bis-(diisopropylphosphino)ethane). In that case, reaction of [Cp*RuCl(dippe)] with $NaBPh_4$ and 1-alkyne in methanol yielded the metastable ruthenium(IV) hydrido–alkynyl complexes [Cp*RuH(C≡CR)(dippe)][BPh_4], whereas addition of 1-alkyne followed by $NaBPh_4$ led to isolation of the corresponding vinylidene derivatives.[3] Trapping of intermediates is due to the insolubility of their [BPh_4]$^-$ salts in methanol (Chart 2). In our case, in the presence of $NaBPh_4$ formation of

Chart 2

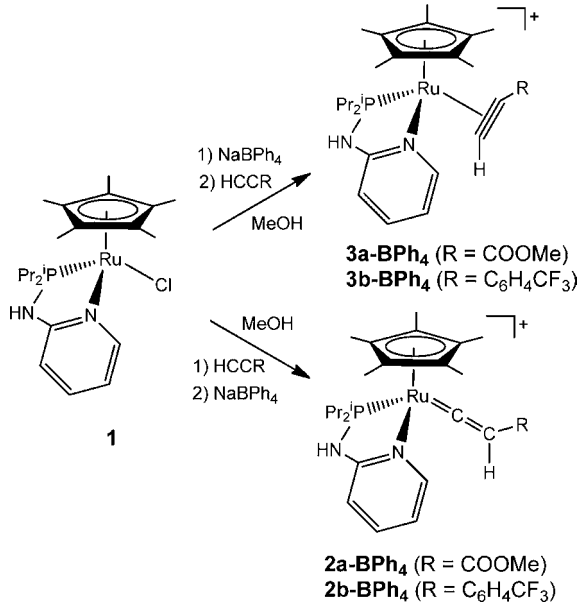

the π-alkyne complexes takes place upon chloride dissociation and salts **3a-BPh$_4$** and **3b-BPh$_4$** precipitate prior to formation of the vinylidene species **2a-BPh$_4$** and **2b-BPh$_4$**, which appear to be more soluble in methanol.

At variance with what has been observed in other cases, π-alkyne derivatives **3a-BPh$_4$** and **3b-BPh$_4$** are stable in the solid state and do not undergo spontaneous rearrangement to vinylidene. Quite surprisingly, isomerization of **3a-BPh$_4$** and **3b-BPh$_4$** to the corresponding vinylidene complexes **2a-BPh$_4$** or **2b-BPh$_4$** is very slow in CD_2Cl_2 at room temperature (Chart 3).

The process is first order with respect to the concentration of π-alkyne complex. The half-life for conversion of **3a-BPh$_4$** into **2a-BPh$_4$** is 6.42 h, whereas in the case of the transformation of **3b-BPh$_4$** into **2b-BPh$_4$** the half-life is 3.85 h. These facts contrast sharply with the observation that **1** reacts directly with 1-alkyne and $NaBPh_4$ in MeOH furnishing the vinylidene complexes through the intermediacy of the π-alkyne adducts (Chart 4).

dx.doi.org/10.1021/ic401119p | Inorg. Chem. 2013, 52, 8919−8932

Chart 3

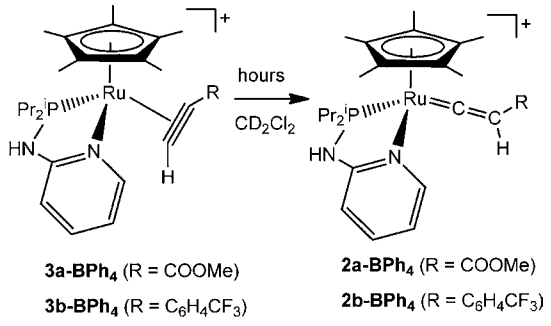

Chart 4

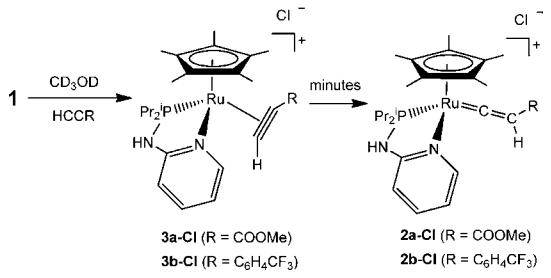

Furthermore, the vinylidene complexes are also accessible by direct reaction of **1** with the corresponding 1-alkyne in dichloromethane, leading to **2a-Cl** and **2b-Cl** in good yields. Under these conditions, formation of the vinylidene complexes occurs even faster in dichloromethane than in methanol. Formation of **2a-Cl** takes place in parallel with a highly exothermic side catalytic reaction of cyclotrimerization of HC≡CCOOMe, leading to mixtures of 1,3,5- and 1,2,4-tris(carboxymethyl)benzene as organic side products.[33]

In order to clarify these apparent contradictions, we monitored by $^{31}P\{^1H\}$ NMR spectroscopy reaction of **1** with an excess of HC≡CR (R = COOMe, $C_6H_4CF_3$) in CD_3OD and CD_2Cl_2. Immediately upon sample preparation we can identify broad resonances in the $^{31}P\{^1H\}$ NMR spectrum attributable to the two diastereomers of the corresponding cationic π-alkyne complex $[Cp^*Ru(HC{\equiv}CR)(^iPr_2PNHPy)]^+$ with chloride as counterion (R = COOMe (**3a-Cl**), $C_6H_4CF_3$ (**3b-Cl**)). These broad resonances begin to disappear gradually. Simultaneously, one singlet signal attributable to formation of the vinylidene complex **2a-Cl** or **2b-Cl** increases its intensity with time.

We measured the rate of formation of the vinylidene complexes by monitoring the decrease of the intensity of the $^{31}P\{^1H\}$ NMR broad resonances attributable to the π-alkyne complexes and the concomitant increase of the intensity of the sharp resonance of the vinylidene complexes as a function of time using the software of the NMR INOVA400 or AGILENT500 spectrometers. The π-alkyne to vinylidene rearrangement process is first order with respect to the concentration of the π-alkyne complex, and the corresponding rate constants (k_{obs}) were determined. In CD_3OD at 298 K, the process **3a-Cl** → **2a-Cl** has a rate constant of $(1.05 \pm 0.03) \times 10^{-3}$ s^{-1}, equivalent to a half-life of $t_{1/2}$ = 11 min. For **3b-Cl** → **2b-Cl**, the rate constant k_{obs} has a value of $(8.5 \pm 0.2) \times 10^{-4}$ s^{-1}, equivalent to a half-life of $t_{1/2}$ = 13.6 min. At the same temperature, the reactions are faster in CD_2Cl_2: k_{obs} is $(3.5 \pm 0.4) \times 10^{-3}$ s^{-1} for **3b-Cl** → **2b-Cl**. We were unable to measure k_{obs} for **3a-Cl** → **2a-Cl** in CD_2Cl_2 due to the occurrence of the highly exothermic catalytic cyclotrimerization reaction of HC≡CCOOMe. In any case, the sharp increase in temperature favors formation of the vinylidene **2a-Cl** within seconds.

We determined the values of k_{obs} for the π-alkyne to vinylidene rearrangement process over a range of temperatures ranging from 273 to 325 K. Listings of rate constants can be found in the Supporting Information. Activation parameters were derived from the corresponding Eyring plots (Figure 2), and the resulting parameters are listed in Table 2.

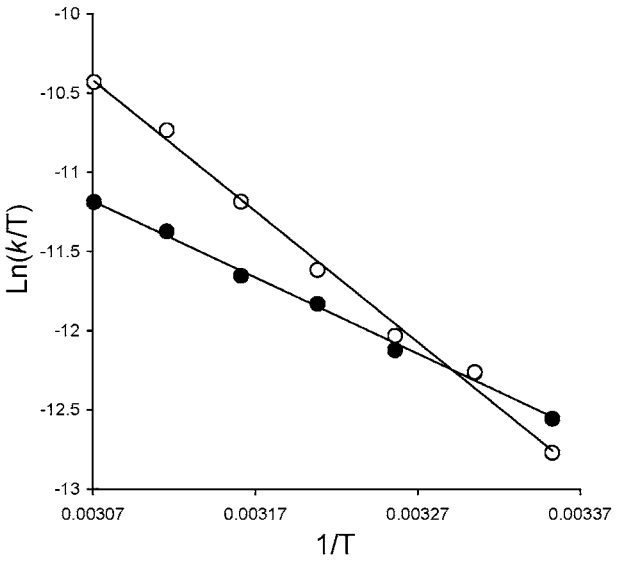

Figure 2. Eyring plots for rearrangement processes **3a-Cl** → **2a-Cl** (●) and **3b-Cl** → **2b-Cl** (○) in CD_3OD.

Table 2. Activation Parameters for Isomerization Processes 3a/b-Cl → 2a/b-Cl in CD_3OD and in CD_2Cl_2

process	solvent	$\Delta H^{\ddagger}$ (kcal mol^{-1})	$\Delta S^{\ddagger}$ (eu)	$\Delta G^{\ddagger}_{298}$ (kcal mol^{-1})
3a-Cl → **2a-Cl**	CD_3OD	9.6 ± 0.3	−40 ± 1	21.5 ± 0.6
	CD_2Cl_2	[a]	[a]	[a]
3b-Cl → **2b-Cl**	CD_3OD	16.4 ± 0.5	−18 ± 2	21.0 ± 1
	CD_2Cl_2	21.1 ± 0.5	0 ± 2	21.1 ± 0.7

[a]Not determined.

The values obtained for $\Delta G^{\ddagger}_{298}$ are essentially identical to those measured for isomerization of the hydrido−alkynyl complexes $[Cp^*RuH(C{\equiv}CR)(dippe)][BPh_4]$ (R = COOMe, Ph, $SiMe_3$, H) to the vinylidene derivatives $[Cp^*Ru{=}C{=}CHR(dippe)][BPh_4]$ ($\Delta G^{\ddagger}_{298}$ = 19−22 kcal mol^{-1}, depending on the group R).[3] They also resemble the values found for isomerization of $[CpRu(HC{\equiv}CMe)(PMe_3)_2]^+$ to $[CpRu{=}C{=}CHMe(PMe_3)_2]^+$ in MeCN ($\Delta G^{\ddagger}_{298}$ = 22 ± 1 kcal mol^{-1}).[2a] Whereas the values for $\Delta H^{\ddagger}$ in our case are rather unexceptional, the largely negative values found for $\Delta S^{\ddagger}$ in CD_3OD contrast with the positive values found for the $[Cp^*RuH(C{\equiv}CR)(dippe)][BPh_4]$ → $[Cp^*Ru{=}C{=}CHR(dippe)][BPh_4]$ rearrangements. Negative activation entropies have been measured for the η^1-*O*-keto alkyne to vinylidene isomerizations, i.e., from $[TpRu\{\eta^1\text{-}O{=}C(R)C{\equiv}CR'\}(^iPr_2PXPy)][BAr'_4]$ to $[TpRu{=}C{=}CR'\{COR\}(^iPr_2PXPy)][BAr'_4]$ (R, R′ = Ph, Me; X = NH, CH_2, S; Ar′ = 3,5-$C_6H_3(CF_3)_2$).[22a] These negative values were interpreted in

dx.doi.org/10.1021/ic401119p | Inorg. Chem. 2013, 52, 8919−8932

terms of a measurement of the decrease of translational, rotational, and vibrational degrees of freedom on the route to the transition state, suggesting a concerted 1,2-sigmatropic shift of the alkyne substituent as the rate-determining step of the reaction. However, for our current situation the large negative values for $\Delta S^{\ddagger}$ may be a sign of an associative-like process during the migration step, suggesting that another species might be involved in the rate-determining transition state.

For comparison purposes, we also determined the activation parameters for rearrangement of the $[BPh_4]^-$ salts **3a/b-BPh$_4$** into their vinylidene isomers **2a/b-BPh$_4$**. As in the previous case, this was achieved by measuring the first-order rate constants for the isomerization process at different temperatures and subsequent representation of the Eyring plots. For this purpose, we had to switch solvent from CD_2Cl_2 to $C_2D_2Cl_4$ (tetrachloethane-d_2) in order to carry out rate constant measurements at temperatures above the boiling point of CD_2Cl_2. From the Eyring plots (see Supporting Information) we calculated the activation parameters shown in Table 3.

Table 3. Activation Parameters for Isomerization Processes 3a/b-BPh$_4$ → 2a/b-BPh$_4$ in Tetrachloroethane-d_2

process	$\Delta H^{\ddagger}$ (kcal mol^{-1})	$\Delta S^{\ddagger}$ (eu)	$\Delta G^{\ddagger}_{298}$ (kcal mol^{-1})
3a-BPh$_4$ → 2a-BPh$_4$	27.8 ± 0.4	9 ± 1	25.1 ± 0.5
3b-BPh$_4$ → 2b-BPh$_4$	23.2 ± 0.4	0 ± 1	23.2 ± 0.7

It can be noticed that the $\Delta G^{\ddagger}_{298}$ values for direct isomerization of the $[BPh_4]^-$ salts in $C_2D_2Cl_4$ are higher than those measured in CD_3OD or CD_2Cl_2 for the chloro derivatives. Furthermore, the enthalpic barriers $\Delta H^{\ddagger}$ are higher, and the entropies are now positive or zero (Table 3), contrasting with the largely negative values found for isomerizations **3a/b-Cl → 2a/b-Cl** in CD_3OD (Table 2). These observations are consistent with the occurrence of alternative reaction pathways for the isomerization processes in each case depending on the nature of the counterion, $[BPh_4]^-$ or Cl^-, as well as the solvent.

In our system, it is now clear that the cationic π-alkyne complexes $[Cp^*Ru(HC{\equiv}CR)(^iPr_2PNHPy)]^+$ (R = COOMe, $C_6H_4CF_3$) are metastable intermediates which undergo a smooth rearrangement to the corresponding vinylidene derivatives. However, this only occurs at a noticeable rate in the presence of chloride, either as a ligand in the precursor complex or as a counterion. If chloride is replaced by $[BPh_4]^-$, then the rearrangement process becomes very slow in CD_2Cl_2. If chloride has indeed an effect on isomerization of the π-alkyne intermediates, an increase in the rate for this process should be expected in the presence of added chloride ion. We measured the isomerization rate of **3a/b-BPh$_4$** to **2a/b-BPh$_4$** in CD_2Cl_2 in the presence of variable amounts of Cl^-. A 1 M stock solution of LiCl in MeOH was prepared. A stoichiometric amount of the crown ether 1,4,7,10,13,16-hexaoxacyclooctadecane (18-crown-6) was added to this solution. The purpose of the addition of the crown ether was to form a macrocyclic chelate complex with the lithium cation in order to minimize its interference with the chloride ion and its active role in the alkyne to vinylidene rearrangement process (i.e., avoid formation of strong $Li^+\cdots Cl^-$ ion pairs in MeOH solution). The required volume of this solution was added via micropipet to a NMR tube containing **3a-BPh$_4$** (25.5 mg, 0.03 mmol) or **3b-BPh$_4$** (28 mg, 0.03 mmol) in CD_2Cl_2. The total volume was 0.6 mL in each case. Formation of vinylidene **2a-BPh$_4$** was monitored by $^{31}P\{^1H\}$ NMR spectroscopy over a period of 100 min. During this time, in the absence of added chloride ion conversion of **3a-BPh$_4$** into **2a-BPh$_4$** was small (18%), albeit more significant in the case of the rearrangement of **3b-BPh$_4$** to **2a-BPh$_4$** (28%). An increase in the isomerization rate was observed in samples with added Cl^-. Isomerization rate constants (first order with respect to the concentration of π-alkyne complex) were determined by analysis of stacked plots of $^{31}P\{^1H\}$ NMR spectra at 298 K. Listings of rate constants can be found in the Supporting Information. Figure 3 shows a plot representing the value of the rate constants for the rearrangement processes **3a-BPh$_4$ → 2a-BPh$_4$** and **3b-BPh$_4$ → 2b-BPh$_4$** against the molar ratio LiCl/π-alkyne complex.

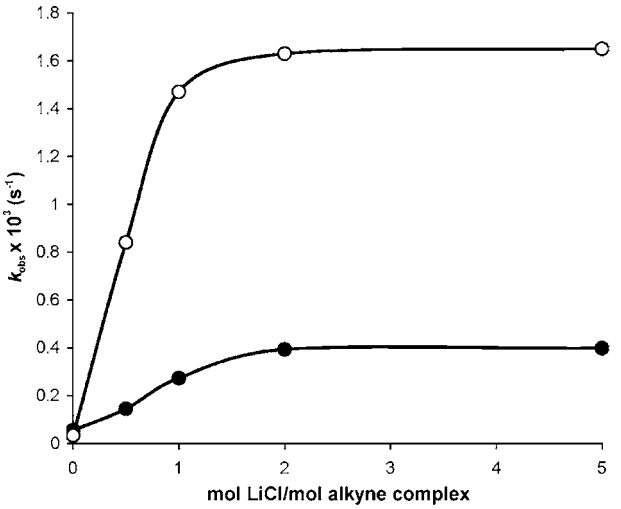

Figure 3. Plot of rate constants for the processes **3a-BPh$_4$ → 2a-BPh$_4$** (○) and **3b-BPh$_4$ → 2b-BPh$_4$** (●) in CD_2Cl_2 at 298 K against the molar ratio LiCl/π-alkyne complex.

The isomerization rate constants increase their values with increasing amounts of LiCl added until a plateau is reached. For **3a-BPh$_4$**, the values for the rate constants range from $(3.30 \pm 0.02) \times 10^{-5}$ s^{-1} in the absence of LiCl to $(1.65 \pm 0.04) \times 10^{-3}$ s^{-1} when the molar ratio LiCl/**3a-BPh$_4$** is 5:1. In the case of **3b-BPh$_4$**, the differences are not so marked but the rate constants still range from $(5.46 \pm 0.06) \times 10^{-5}$ s^{-1} in the absence of LiCl to $(3.98 \pm 0.08) \times 10^{-4}$ s^{-1} when the molar ratio LiCl/**3b-BPh$_4$** is 5:1. This experiment indicates that chloride may play an active role in the alkyne to vinylidene isomerization processes under study. However, since MeOH is the solvent used for the LiCl/crown ether solution, the possibility that methanol molecules might also participate in the isomerization process should be taken into account. In order to examine this hypothesis, we carried out experiments in which we added 100 μL of neat MeOH to a NMR tube containing **3a-BPh$_4$** (25.5 mg, 0.03 mmol) or **3b-BPh$_4$** (28 mg, 0.03 mmol) in CD_2Cl_2, and then the isomerization rates were measured in the usual way. For the process **3a-BPh$_4$ → 2a-BPh$_4$**, the value for the observed rate constant was $(2.5 \pm 0.1) \times 10^{-4}$ s^{-1}, whereas for **3b-BPh$_4$ → 2b-BPh$_4$** a value of $(1.92 \pm 0.04) \times 10^{-4}$ s^{-1} was obtained. These rate constants indicate that the isomerization process indeed occurs faster in the presence of MeOH alone, although slower than in the presence of added LiCl. These observations suggest that both the chloride ion as well as MeOH play active roles in the alkyne to vinylidene isomerization process in these complexes. In order to understand the

dx.doi.org/10.1021/ic401119p | Inorg. Chem. 2013, 52, 8919−8932

function of chloride and MeOH in the overall rearrangement, a computational study has been carried out to propose feasible reaction pathways.

Computational Study. *Theoretical Models and Mechanistic Considerations.* Calculations have been performed using the actual ruthenium complex [Cp*RuCl(^{i}Pr$_2$PNHPy)], with no simplifications in the ligands' framework, and the alkyne HC≡CR where R = COOMe. From the experimental study (Tables 2 and 3), a similar behavior could be expected for the substrate containing the group *p*-$C_6H_4CF_3$. As shown in the experimental study, the π-alkyne complexes are initial intermediates for isomerization. Similarly to what we found for the vinylidene complexes (Figure 1), π-alkyne complexes are also much more stable as a tight ion pairs with chloride than with a coordinated chloride replacing the nitrogen ligand. We considered the ion-paired π-alkyne complexes [Cp*Ru(HC≡CR)(^{i}Pr$_2$PNHPy)]Cl (R = COOMe, **3a-Cl**) as the initial species in the isomerization process. The relative energy of **1** + HC≡CCOOMe with respect to **3a-Cl** is 11.4 kcal mol^{-1}. In order to properly describe the ion pairs, all intermediates and transition states were optimized in solvent conditions through a continuum description of the methanol solvent. In selected cases, explicit methanol molecules were included in the calculations. All energies reported correspond with Gibbs energies in methanol in kcal mol^{-1}.

Several intramolecular mechanisms for the alkyne to vinylidene isomerization have been investigated in the presence of the chloride anion (1,2- and 1,3-hydrogen shifts, Scheme 2).

Scheme 2. Mechanisms Theoretically Studied for the Alkyne to Vinylidene Isomerization

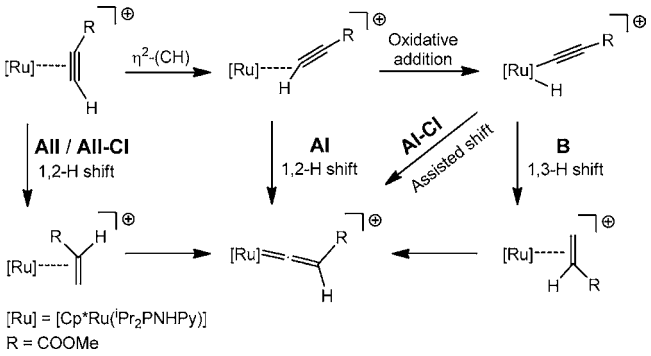

Previous theoretical works showed that the 1,2-hydrogen path in Ru(II) d^6 complexes occurs through a preliminary slippage process to a η^2-(C−H) intermediate and subsequent 1,2-H migration from C_α to C_β (pathway **AI**), whereas rearrangement from the π-alkyne complex is unlikely to proceed (pathway **AII**).[7d,24] On the other hand, the 1,3-H migration (pathway **B**) entails oxidative addition of the coordinated alkyne to give a hydrido−alkynyl complex, which then isomerizes via 1,3-H shift. The influence of the chloride anion in these routes has been considered, namely, pathways **AI-Cl** and **AII-Cl** (stable intermediates in pathway **B** were not found). As a result, the anion behaves innocently in **AII-Cl** but performs an active role in **AI-Cl**.

η^2-(C−H) vs Hydrido−Alkynyl Intermediates. The 1,2-H migration in pathway **AII** occurs starting from the π-alkyne intermediate. However, the 1,2- and 1,3-H migrations for pathways **AI** and **B** migrations imply different intermediates: a η^2-(C−H) alkyne participates in the former (**AI**), whereas a hydrido−alkynyl complex is required for the latter (**B**). For both pathways the first step of the mechanism involves the change from η^2-CC to a η^2-(C−H) coordination mode in order to activate the C−H bond of the terminal alkyne. Therefore, we initially studied the formation and relative stability of η^2-(C−H) and hydrido−alkynyl intermediates. Throughout this study the chloride anion is placed at the surrounding of the NH linking group as an ion pair forming a Cl···H−N hydrogen bond (Figure 1A). Complex **3a-Cl** exists as a mixture of two diastereomers resulting from the two possible orientations of the π-alkyne ligand with respect to the phosphorus and pyridyl groups bound to ruthenium (**I** and **II**, Chart 1). **I** describes the rotamer with the alkyne hydrogen atom closer to the phosphine ligand, whereas diastereomer **II** locates it on the pyridine side. Both diastereomers have similar stabilities in agreement with NMR detection of a mixture of both. The most stable π-alkyne rotamer **II-3a-Cl** was taken as our zero or energies (Scheme 3). We studied the further evolution of both **I** and **II** diastereomers of **3a-Cl** (Scheme 3). Rearrangement of the π-alkyne toward a η^2-(C−H) coordination mode involves moderate barriers: the transition states describing such coordination change, **I-TS3a-5a-Cl** and **II-TS3a-4a-Cl**, are located 26.4 and 27.4 kcal mol^{-1} above **II-3a-Cl**. In order to analyze whether the chloride anion can assist the rearrangement, the chloride anion was located close to the alkyne ligand, forming a weak hydrogen bond interaction with the acidic alkyne hydrogen. The resulting complexes **I-3a-Cl′** and **II-3a-Cl′** are less stable, and the energy to reach the corresponding transition states for the coordination change, **I-TS3a-5a-Cl′** and **II-TS3a-4a-Cl′**, are 27.1 and 27.8 kcal mol^{-1}, respectively. Therefore, the presence of the chloride anion in this moiety does not influence the π-alkyne → η^2-(C−H) rearrangement. Nevertheless, the process can take place by means of a less energy demanding stepwise dissociative−associative process. The unsaturated ruthenium complex and the alkyne reactant were computed separately (**0a-Cl**) showing a relative Gibbs energy of 11.9 kcal mol^{-1} (the relative energy in solution, ΔE_{MeOH}, is 27.0 kcal mol^{-1}). Static calculations cannot afford a good approach for entropic contributions in dissociative processes; thus, the Gibbs energy of **0a-Cl** can be only considered as an estimation of the activation barrier.[34] For system **II**, subsequent association leads η^2-(C−H) intermediate **II-4a-Cl** which evolves in an essentially barrierless process (**II-TS-4a-5a-Cl**) to the most stable hydrido−alkynyl complex **II-5a-Cl**.[35] For system **I**, the η^2-(C−H) intermediate has not been found;[36] instead, optimization leads directly to the hydrido−alkynyl complex **I-5a-Cl**. This intermediate is only 4.5 kcal mol^{-1} less stable than reactants; therefore, although it can be hardly detected, it can participate as transient species in further steps. No stable ion pairs of chloride with the hydrogen atom were found involving σ (**4a**) or hydrido (**5a**) complexes.

Overall, the theoretical study of the first step of the isomerization process outlines the feasibility of hydrido−alkynyl species as intermediates. This result contrasts with previous theoretical studies on ruthenium systems in which the η^2-(C−H) intermediate was found to be much more stable than the hydrido−alkynyl complex resulting from oxidative addition.[7b,8,9] The most basic nature of the ligands in our system increases the stability of the ruthenium(IV) hydrido−alkynyl complex and destabilizes the η^2-(C−H) intermediate.

H-Migration Step. The migration step has been computationally studied using both diastereomers, but only system **I** will be shown here since it has the lowest activation barriers. The

dx.doi.org/10.1021/ic401119p | Inorg. Chem. 2013, 52, 8919−8932

Scheme 3. Proposed Mechanisms for Formation of Hydrido−Alkynyl Complexes (R = COOMe)[a]

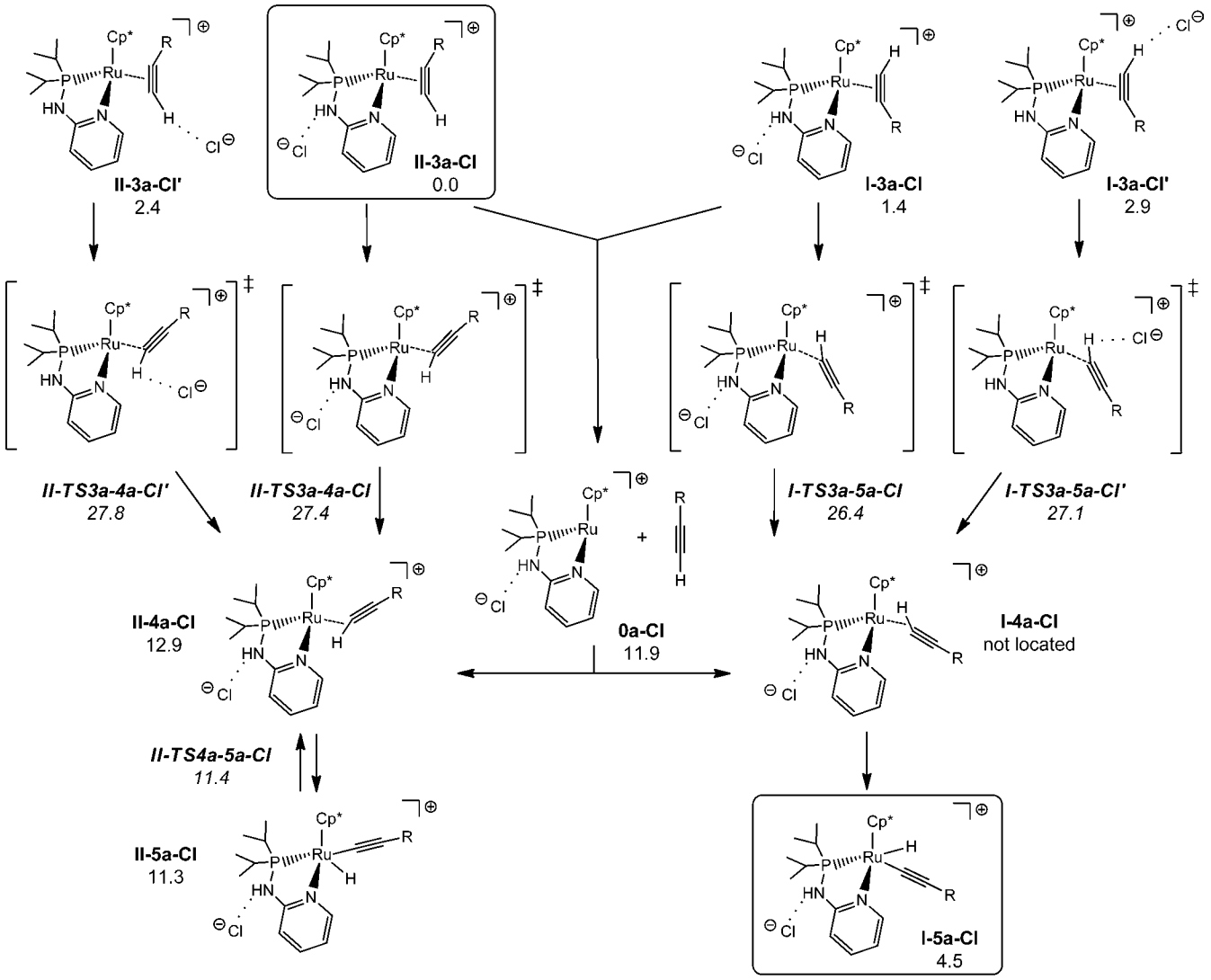

[a]Relative Gibbs energies in methanol in kcal mol^{-1}.

more feasible routes using the other diastereomer (system **II**) can be found in the Supporting Information. In order to make the reading easier, hereupon the notation for system **I** will be deliberately omitted.

During the first part of the study, the chloride anion was treated as a spectator species. In this regard, Scheme 4 shows the calculated isomerization mechanisms. Starting from a π-alkyne species, the 1,2-H migration **AII** can be described via **TS3a-6a-Cl**. The activation barrier is 48.8 kcal mol^{-1}, and the η^2-vinylidene **6a** is placed at 32.8 kcal mol^{-1} above **II-3a-Cl**. Due to the large energy barrier obtained, the following isomerization steps were not evaluated. For the 1,2-H migration via pathway **AI**, the reaction should begin with the hydrido−alkynyl **5a-Cl** since the η^2-(C−H) intermediate could not be located for system **I** (Scheme 3). The concerted transition state **TS5a-2a-Cl** involves a 1,3-H shift, which demands 30.5 kcal mol^{-1}. The vinylidene product **2a-Cl** is found 14.3 kcal mol^{-1} below **II-3a-Cl**. Finally, pathway **B** also entails a 1,3-H migration through **TS5a-7a′-Cl** and **TS7a′-7a-Cl** involving 39.0 and 38.0 kcal mol^{-1}, respectively. The resulting agostic species **7a-Cl** is not a feasible intermediate since it is placed at 37.3 kcal mol^{-1} above reactants; thus, further conformational events to form the final product were omitted. In summary, the Gibbs energy barrier of pathway **AI** (30.5 kcal mol^{-1}) is lower than that of routes **AII** and **B** but still higher than the experimental value (21.5 kcal mol^{-1}, see Table 2). The transition state structure **TS5a-2a-Cl** (Figure 4, left) is similar to that calculated for the 1,2-H shift from [RhCl(PH$_3$)$_2$(H)-(C≡CH)] to [RhCl(PH$_3$)$_2$(=C=CH$_2$)].[7c]

In previous studies the chloride anion has played a spectator role, only forming an ion pair with the ruthenium complex. The following calculations, depicted in Scheme 5, show the active role of such an anion during the migration processes, i.e., pathways **AII-Cl** and **AI-Cl**. Both routes involve migration of a chloride anion from the ligand N−H side to the alkyl C−H side. The cost of this initial reorganization cannot be properly evaluated with the solvent model we are using and has not been computed. For pathway **AII-Cl**, the transition state **TS3a-6a-Cl′** describes the 1,2-H migration involving 51.3 kcal mol^{-1}. The chloride interacts with the migrating hydrogen, but no diminution of the activation barrier was found. On the other hand, i.e., pathway **AI-Cl**, the chloride abstracts the hydrogen of

dx.doi.org/10.1021/ic401119p | Inorg. Chem. 2013, 52, 8919−8932

Scheme 4. Calculated Mechanisms for Alkyne to Vinylidene Isomerization (R = COOMe)[a]

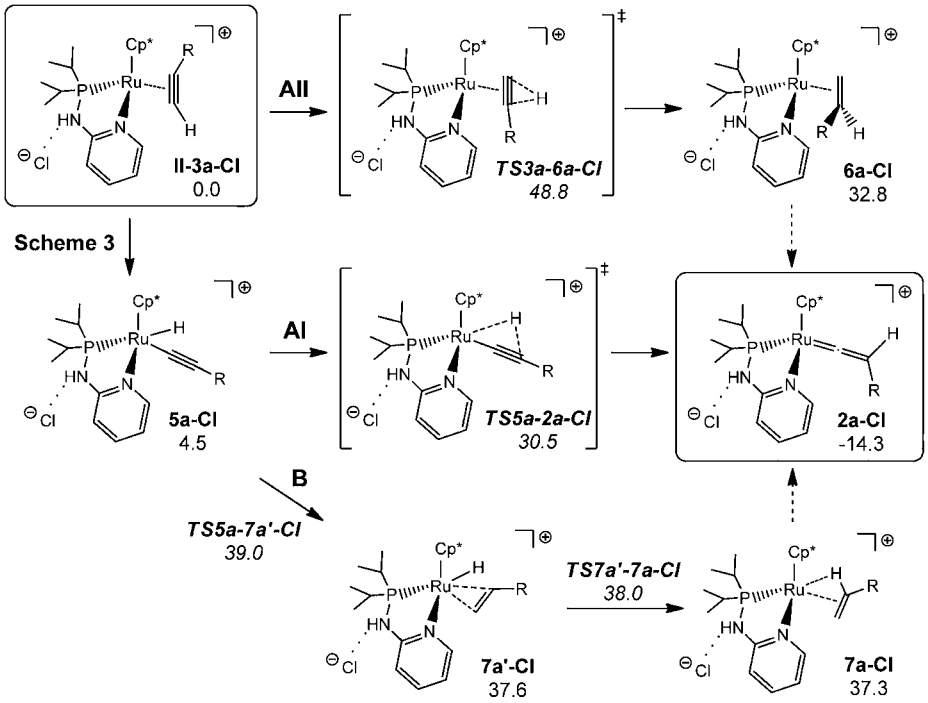

[a]Relative Gibbs energies in methanol in kcal mol^{-1}.

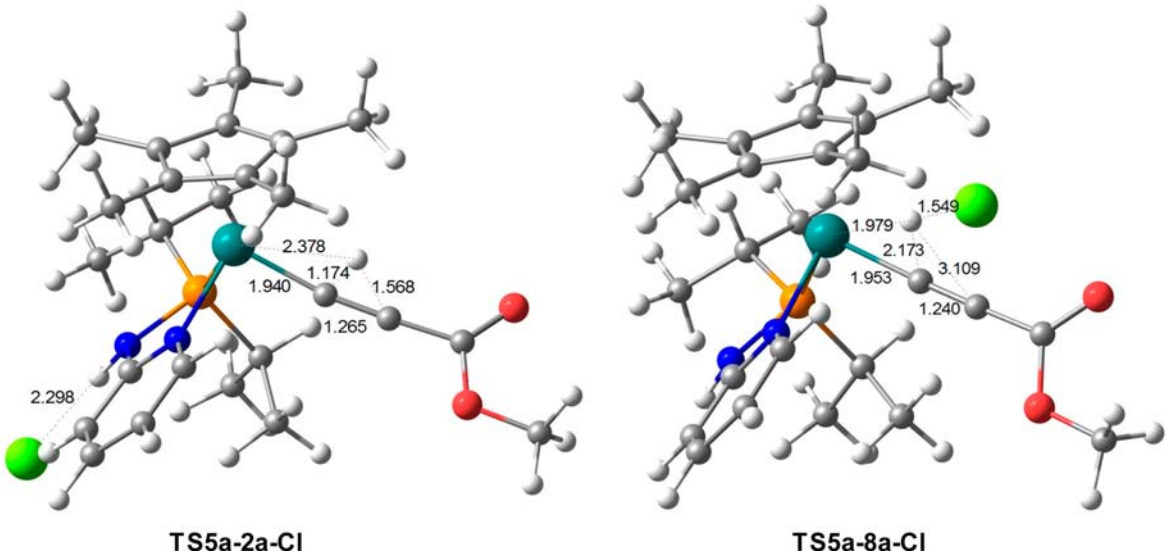

Figure 4. Optimized structures of transition states **TS5a-2a-Cl** (left) and **TS5a-8a-Cl** (right). Bond distances in Angstroms.

5a-Cl as a proton via **TS5a-8a-Cl** (Figure 4, right); the Gibbs energy barrier significantly decreases to 16.7 kcal mol^{-1}. Then, from **8a-Cl** the proton is shuttled to the β-carbon, yielding the vinylidene complex **2a-Cl**. The relative Gibbs energy of the transition state for this proton transfer (**TS8a-2a-Cl**) is 17.4 kcal mol^{-1}, similar to the previous step.[37] This reaction shortcut powered by the anion prevents formation of unstable intermediates, and therefore, the reaction rate is increased. Nevertheless, this value is underestimated according to the experimental one, i.e., 21.5 kcal mol^{-1}. Even performing all of the optimizations in solution, the description of the chloride behavior in methanol solution with only a continuum model for the solvent could be a rather simple model to account for the operating mode of this anion. We will come back to this point later on.

A counteranion acting as a proton shuttle has been identified in other proton transfer processes.[25−28] Additionally, a ligand-assisted proton shuttle (LAPS) mechanism was recently proposed for the alkyne to vinylidene isomerization mediated by the complex [Ru(κ^2-OAc)$_2$(PPh$_3$)$_2$], in which the acetate ligand facilitates migration of the alkyne proton via intramolecular deprotonation/protonation.[38]

Deprotonation of the hydrido−alkynyl intermediate by the chloride anion should imply a notable acidic character on the hydrido ligand. To check this hypothesis, we calculated the pK_a^{MeOH} of the hydrido ligand of **5a-Cl** using the thermody-

dx.doi.org/10.1021/ic401119p | Inorg. Chem. 2013, 52, 8919−8932

Scheme 5. Cl-Assisted Calculated Mechanisms for Alkyne to Vinylidene Isomerization (R = COOMe)[a]

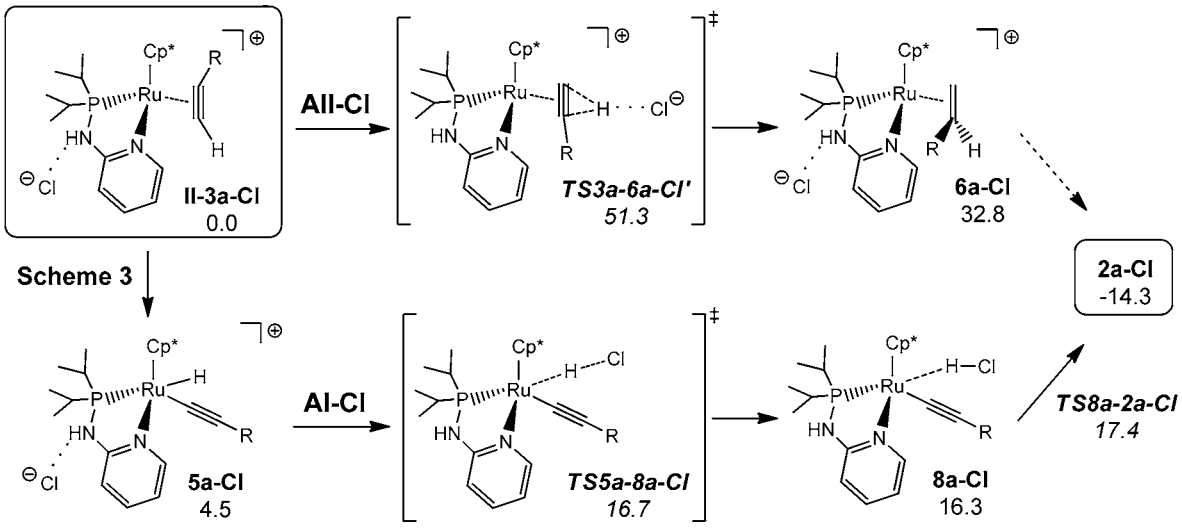

[a]Relative Gibbs energies in methanol in kcal mol^{-1}.

Scheme 6. Base-Assisted H-Migration Step (R = COOMe) for Pathway AI-B Including Two Methanol Solvent Molecules[a]

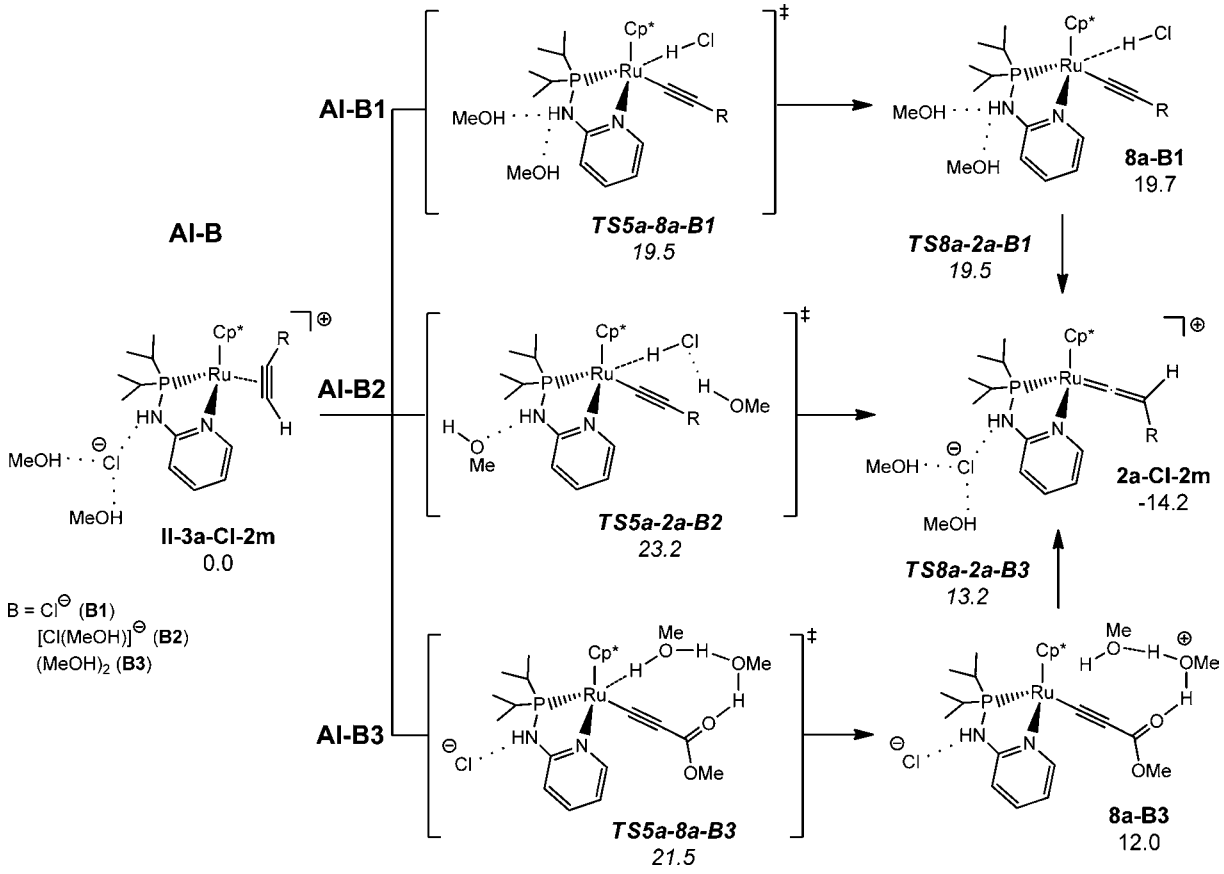

[a]Relative Gibbs energies in methanol in kcal mol^{-1}.

namic cycle involving a mixed continuum-cluster model[39] that has been already employed for estimation of pK_a values of organometallic complexes (see Supporting Information for details and M06 calculations).[24,40] The computed value of 1.1 suggests that the hydrido ligand exhibits a relatively strong acid character which reinforces the availability of the Cl-assisted deprotonation step.[41] In this regard, any species with enough basic character to abstract the hydrogen atom in **5a-Cl** could play the role of the chloride. As pointed out by experiments, methanol solvent molecules are indeed good candidates for such duty.

To back up counteranion and solvent influence into the proton-migration step, two methanol molecules were explicitly included in the calculations. Recent theoretical studies have

dx.doi.org/10.1021/ic401119p | Inorg. Chem. 2013, 52, 8919−8932

shown that at least two alcohol molecules are required to assist proton migration processes.[42] Using this improved description of the experimental conditions, the migration step (**AI-B**) was computed using Cl^- (**AI-B1**), $[Cl(MeOH)]^-$ (**AI-B2**), and $(MeOH)_2$ (**AI-B3**) species as promoting agents (Scheme 6). Analogously to the **AI-Cl** mechanism (Scheme 5), pathway **AI-B1** describes the Cl-assisted migration (**TS5a-8a-B1** and **TS8a-2a-B1**) through intermediate **8a-B1** located at 19.7 kcal mol^{-1}. The vinylidene product **2a-Cl-2m** is found at 14.2 kcal mol^{-1} below reactant **II-3a-Cl-2m**. The basic character of the chloride anion is decreased by inclusion of one methanol molecule in its solvation sphere, i.e., pathway **AI-B2**. Accordingly, the Gibbs energy barrier for migration increases to 23.2 kcal mol^{-1} (**TS5a-2a-B2**). For this particular case, the process was found to be concerted. Finally, direct implication of solvent molecules was evaluated for pathway **AI-B3**. Transition state **TS5a-8a-B3** shows two methanol molecules forming a hydrogen-bonded chain between the hydride and the COOMe group of the alkynyl ligand (Figure 5), in a similar way to the transition

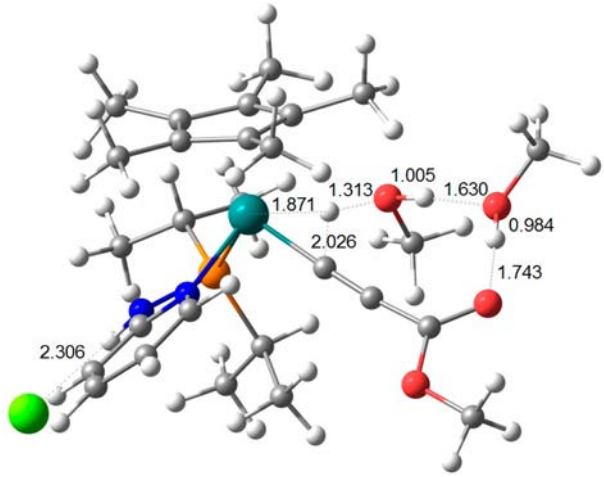

Figure 5. Optimized structure of transition state **TS5a-8a-B3**. Bond distances in Angstroms.

states described in Au(I)-catalyzed alcohol addition reactions.[42] The deprotonation process entails 21.5 kcal mol^{-1} and generates intermediate **8a-B3** in which the positive charge is placed at one oxygen atom forming a $MeOH_2^+$ species. Then, the proton is easily transferred to the β-carbon, yielding the vinylidene product **2a-Cl-2m**. As pointed out above, a continuum or a cluster solvent model with a limited number of solvent molecules cannot give a good estimation of the energetic cost of the chloride and methanol migrations between the NH ligand side and the alkyl side that happen between **II-3a-Cl-2m** and the various transition states shown in Scheme 6. Nevertheless, we expect this issue will not impact dramatically the outcome in actual solution conditions. Overall, the calculated Gibbs energy barriers are close to the one experimentally reported in methanol solution (21.5 kcal mol^{-1}, see Table 2), supporting the viability of the base-assisted mechanism. Additionally, the negative $\Delta S^{\ddagger}$ values found for this reaction (Table 2) could be related with the intermolecular mechanism disclosed by the calculations. Although in the calculations the number of species does not change along the process, a tighter arrangement in the transition states should imply negative entropies.

In summary, the computational results obtained for the alkyne HC≡CR (R = COOMe) show that pathways **AII** and **B** can be discarded. Nevertheless, pathway **AI** still exhibits a large Gibbs energy barrier. The chloride anion directly influences the migration process via pathway **AI-Cl** involving the hydrido−alkynyl complex **5a-Cl**. The chloride takes the hydrogen from the metal to place it at the β-carbon, forming the vinylidene product, acting as proton shuttle. The acidic character of **5a-Cl** favors other species, such as methanol solvent molecules, being able to assist the H-migration step. In other words, species capable to act as weak bases (namely, **B**) can assist the process (pathway **AI-B**). Finally, assuming that formation of the hydrido−alkynyl **5a-Cl** is not the rate-determining step, the calculated Gibbs energy barriers via **AI-B** are in line with the experimental value measured in methanol (21.5 kcal mol^{-1}). It is worth mentioning that the most important point that arises from the calculations is not the factual reproduction of the experimental value that may result from cancellation of errors but the evidence of a feasible influence of external species in the isomerization process.

■ CONCLUSIONS

In the present work the counteranion and solvent assistance in Ru-mediated alkyne to vinylidene isomerizations have been disclosed. Experimental studies demonstrate that the reaction, which involves metastable π-alkyne adducts, is sensitive to the counteranion present. Isomerization takes place in hours in the presence of $[BPh_4]^-$ as counteranion or in minutes if Cl^- is present. The kinetic study also shows a remarkable increase in reaction rates by addition of LiCl in methanol solution. DFT calculations were carried out to investigate the mechanistic scenario. In methanol solution, the calculated 1,2-hydrogen (**AI** and **AII**) and 1,3-hydrogen (**B**) shifts exhibit rather high Gibbs energy barriers. However, participation of a hydrido−alkynyl complex during the isomerization process can be envisaged. Due to the acidic character of this intermediate, basic species can act as proton shuttles, assisting the 1,3-H shift (**AI-Cl** and **AI-B**). Indeed, participation of external molecules during the isomerization process is computationally supported.

■ EXPERIMENTAL SECTION

All synthetic operations were performed under a dry dinitrogen or argon atmosphere following conventional Schlenk techniques. Tetrahydrofuran, diethyl ether, and petroleum ether (boiling point range 40−60 °C) were obtained in the oxygen- and water-free from an Innovative Technology, Inc. solvent purification apparatus. Dichloromethane and methanol were of anhydrous quality and used as received. All solvents were deoxygenated immediately before use. Diisopropylphosphinyl-2-pyridylamine and the complex [Cp*RuCl-(^{i}Pr$_2$PNHPy)] were prepared according to reported procedures.[29,43] IR spectra were recorded in Nujol mulls with a Perkin−Elmer FTIR Spectrum 1000 spectrophotometer. NMR spectra were taken on Varian Inova 400 MHz, Agilent 400MR, Agilent DD2 500 MHz ,or Varian Inova 600 MHz equipment. Chemical shifts are given in ppm from $SiMe_4$ (^{1}H and $^{13}C\{^1H\}$), 85% H_3PO_4 ($^{31}P\{^1H\}$), or fluorobenzene (^{19}F). ^{1}H and $^{13}C\{^1H\}$ NMR spectroscopic signal assignments were confirmed by ^{1}H-gCOSY, DEPT, and gHSQC (^{1}H−^{13}C) experiments when required. Microanalyses were performed with a LECO CHNS-932 elemental analyzer at the Servicio Central de Ciencia y Tecnología, Universidad de Cádiz. Conductivity measurements were carried out with a Crison 524 conductimeter in nitromethane solutions.

[Cp*Ru=C=CHR(^{i}Pr$_2$PNHPy)][Cl] (R = COOMe (2a-Cl), $C_6H_4CF_3$ (2b-Cl)). To a solution of [Cp*RuCl(^{i}Pr$_2$PNHPy)] (0.24 g, 0.5 mmol) in dichloromethane (8 mL), a slight excess over the

dx.doi.org/10.1021/ic401119p | Inorg. Chem. 2013, 52, 8919−8932

stoichiometric amount of the corresponding alkyne HC≡CR (R = COOMe, $C_6H_4CF_3$) was added. The mixture was stirred at room temperature for 1 h. At the end of this time, the solvent was removed in vacuo and the resulting solid washed with petroleum ether until a microcrystalline solid was obtained and then dried in vacuo. Data for **2a-Cl**: Yield 0.26 g, 95%. Anal. Calcd for $C_{25}H_{38}N_2ClO_2PRu$: C, 53.0; H, 6.77; N, 4.9. Found: C, 53.4; H, 6.84; N, 4.8. IR (Nujol, cm^{-1}): ν(NH) 3376; ν(CO) 1681; ν(CN) 1593. ^1H NMR (400 MHz, CD_2Cl_2, 298 K): δ 1.00, 1.11, 1.19, 1.47 (m, 3 H each, $P(CH(CH_3)_2)_2$), 1.83 (s, 15 H, $C_5(CH_3)_5$), 2.20, 2.97 (m, 1 H each, $P(CH(CH_3)_2)_2$), 3.48 (s, 3 H, $COOCH_3$), 4.50 (s, 1 H, RuC=CH), 6.49 (t, 1 H), 7.29 (d, 1 H), 7.43 (t, 1 H), 7.66 (d, 1H) (C_5H_4N), 10.8 (s br, 1 H, NH). $^{31}P\{^1H\}$ NMR (161.89 MHz, CD_2Cl_2, 298 K): δ 133.5 (s). $^{13}C\{^1H\}$ NMR (100.57 MHz, $CDCl_3$, 298 K): δ 10.4 (s, $C_5(CH_3)_5$), 17.0, 17.4, 18.1, 18.3 (s, $P(CH(CH_3)_2)_2$), 28.9 (d, $^1J_{CP}$ = 24 Hz, $P(CH(CH_3)_2)$), 29.9 (d, $^1J_{CP}$ = 37 Hz, $P(CH(CH_3)_2)$), 51.2 (s, $COOCH_3$), 103.0 (s, $C_5(CH_3)_5$), 112.8 (s, Ru=C=CH), 108.6 (s), 115.1 (s), 139.1 (s), 151.9 (s), 164.3 (d) (C_5H_4N), 166.2 (s, $COOCH_3$), 340.3 (s br, Ru=C). Data for **2b-Cl**: Yield 0.29 g, 90%. Anal. Calcd for $C_{30}H_{39}N_2ClF_3PRu$: C, 55.3; H, 6.03; N, 4.3. Found: C, 55.4; H, 6.09; N, 4.2. IR (Nujol, cm^{-1}): ν(NH) 3386; ν(CC) + ν(CN) 1609(sh), 1596. ^1H NMR (400 MHz, $CDCl_3$, 298 K): δ 0.92, 1.13, 1.19, 1.37 (m, 12 H, $P(CH(CH_3)_2)_2$), 1.75 (s, 15 H, $C_5(CH_3)_5$), 2.21, 2.98 (m, 1 H each, $P(CH(CH_3)_2)_2$), 5.03 (s, 1 H, RuC=CH), 6.65, 7.22 (d, $^3J_{HH}$ = 8.2 Hz, 2 H each, $C_6H_4CF_3$), 6.54 (t, 1H), 7.34 (t, 1 H), 7.40 (d, 1 H), 7.68 (d, 1H) (C_5H_4N), 10.8 (s br, 1 H, NH). $^{31}P\{^1H\}$ NMR (161.89 MHz, $CDCl_3$, 298 K): δ 134.2 (s). $^{13}C\{^1H\}$ NMR (100.57 MHz, $CDCl_3$, 298 K): δ 10.6 (s, $C_5(CH_3)_5$), 16.8, 17.4, 17.8, 18.5 (s, $P(CH(CH_3)_2)_2$), 29.4 (d, $^1J_{CP}$ = 21.4 Hz, $P(CH(CH_3)_2)$), 30.2 (d, $^1J_{CP}$ = 37.8 Hz, $P(CH(CH_3)_2)$), 102.4 (s, $C_5(CH_3)_5$), 116.4 (s, Ru=C=CH), 112.6 (s), 115.5 (s), 138.7 (s), 151.2 (s), 164.4 (d) (C_5H_4N), 124.1, 125.2, 134.5 (s, $C_6H_4CF_3$), 127.1 (q, $^1J_{CF}$ = 32.7 Hz, $C_6H_4CF_3$), 346.1 (s br, Ru=C). ^{19}F NMR (376.26 MHz, $CDCl_3$, 298 K): δ −62.7 (s).

[Cp*Ru=C=CHR(^{i}Pr$_2$PNHPy)][BPh$_4$] (R = COOMe (2a-BPh$_4$), C$_6$H$_4$CF$_3$ (2b-BPh$_4$)). To a solution of **2a-Cl** (0.25 g, 0.44 mmol) or **2b-Cl** (0.25 g, 0.38 mmol) in MeOH (8 mL), an excess amount of solid $NaBPh_4$ (0.2 g, ca. 0.6 mmol) was added. The mixture was stirred for 2 h. A yellow or pink precipitate was obtained. It was filtered, washed with EtOH and petroleum ether, and dried in vacuo. Products were recrystallized from acetone/ethanol or dichloromethane/ethanol mixtures. Data for **2a-BPh$_4$**: Yield 0.28 g, 76%. Anal. Calcd for $C_{49}H_{58}N_2BO_2PRu$: C, 69.3; H, 6.88; N, 3.3. Found: C, 69.5; H, 6.99; N, 3.1. IR (Nujol, cm^{-1}): ν(NH) 3384; ν(CO) 1732; ν(CN) + ν(C=C) 1688, 1595. ^1H NMR (400 MHz, CD_2Cl_2, 298 K): δ 0.87, 1.03, 1.08, 1.18 (m, 3 H each, $P(CH(CH_3)_2)_2$), 1.83 (d, 15 H, $C_5(CH_3)_5$), 2.21, 2.77 (m, 1 H each, $P(CH(CH_3)_2)_2$), 3.46 (s, 3 H, $COOCH_3$), 4.10 (d, J_{HP} = 1 Hz, 1 H, RuC=CH), 5.77 (d, J_{HP} = 3 Hz, 1 H, NH), 6.55 (d, 1 H), 6.62 (t, 1 H), 7.15 (t, 1 H), 7.25 (d, 1 H) (C_5H_4N). $^{31}P\{^1H\}$ NMR (161.89 MHz, CD_2Cl_2, 298 K): δ 135.3 (s). $^{13}C\{^1H\}$ NMR (100.57 MHz, CD_2Cl_2, 298 K): δ 10.9 (s, $C_5(CH_3)_5$), 16.9 (d), 17.4 (d), 17.8 (d), 18.9 (d) ($P(CH(CH_3)_2)_2$), 30.0 (d, $^1J_{CP}$ = 19 Hz, $P(CH(CH_3)_2)$), 30.9 (d, $^1J_{CP}$ = 35 Hz, $P(CH(CH_3)_2)$), 52.8 (s, $COOCH_3$), 102.0 (s, $C_5(CH_3)_5$), 110.3 (d), 116.9 (d), 139.7 (s), 153.0 (s), 161.7 (d) (C_5H_4N), 114.4 (s, Ru=C=CH), 165.4 (s, $COOCH_3$), 344.9 (d, J_{CP} = 16 Hz, Ru=C). **2b-BPh$_4$**: Yield 0.28 g, 80%. Anal. Calcd for $C_{54}H_{59}N_2BF_3PRu$: C, 69.3; H, 6.35; N, 3.0. Found: C, 69.1; H, 6.29; N, 2.9. IR (Nujol, cm^{-1}): ν(NH) 3317; ν(CN) + ν(C=C) 1601, 1625. ^1H NMR (400 MHz, CD_2Cl_2, 298 K): δ 0.91, 1.13, 1.17, 1.20 (m, 3 H each, $P(CH(CH_3)_2)_2$), 1.83 (s, 15 H, $C_5(CH_3)_5$), 2.21, 2.71 (m, 1 H each, $P(CH(CH_3)_2)_2$), 5.23 (d, J_{HP} = 1.2 Hz, 1 H, RuC=CH), 5.24 (d br, J_{HP} = 2.9 Hz, 1 H, NH), 6.77, 7.41 (d, $^3J_{HH}$ = 8.2 Hz, 2 H each, $C_6H_4CF_3$), 6.46 (d, 1H), 6.75 (t, 1 H), 7.42 (t, 1 H), 7.56 (d, 1H) (C_5H_4N). $^{31}P\{^1H\}$ NMR (161.89 MHz, CD_2Cl_2, 298 K): δ 136.3 (s). $^{13}C\{^1H\}$ NMR (100.57 MHz, $CDCl_3$, 298 K): δ 10.6 (s, $C_5(CH_3)_5$), 16.0 (d), 16.9 (d), 17.4 (s), 18.3 (s) ($P(CH(CH_3)_2)_2$), 29.0 (d, $^1J_{CP}$ = 19.6 Hz, $P(CH(CH_3)_2)$), 29.9 (d, $^1J_{CP}$ = 35.4 Hz, $P(CH(CH_3)_2)$), 102.9 (d, J_{CP} = 2.5 Hz, $C_5(CH_3)_5$), 116.9 (s, Ru=C=CH), 111.7 (s), 116.7 (s), 139.9 (s), 151.5 (s), 161.6 (d) (C_5H_4N), 124.6, 125.6, 134.0 (s, $C_6H_4CF_3$), 127.1 (q, $^1J_{CF}$ = 32.7 Hz, $C_6H_4CF_3$), 347.8 (d, $^2J_{CP}$ = 15.2 Hz, Ru=C). ^{19}F NMR (376.26 MHz, CD_2Cl_2, 298 K): δ −63.0 (s).

[Cp*Ru(η^2-HC≡CR)(^{i}Pr$_2$PNHPy)][BPh$_4$] (R = COOMe (3a-BPh$_4$), C$_6$H$_4$CF$_3$ (3b-BPh$_4$)). To a solution of **1** (0.3 g, 0.62 mmol) in 8 mL of MeOH at 0 °C (ice bath), solid $NaBPh_4$ (0.3 g, excess) was added. Then, a slight excess over the stoichiometric amount of the corresponding alkyne HC≡CR (R = COOMe, $C_6H_4CF_3$) was added using a micropipet. The mixture was stirred at 0 °C for 30 min. At the end of this time, a yellow microcrystalline precipitate was obtained. It was filtered, washed with EtOH and petroleum ether, and dried in vacuo. In order to remove NaCl, the product was dissolved in the minimum amount of dichloromethane and the yellow solution filtered. Pure product was isolated upon concentration and precipitation with petroleum ether. Data for **3a**: Yield: 0.45 g, 84%. Anal. Calcd for $C_{49}H_{58}N_2BO_2PRu$: C, 69.3; H, 6.88; N, 3.3. Found: C, 69.0; H, 6.76; N, 3.0. IR (Nujol, cm^{-1}): ν(NH) 3314; ν(C≡C) 1838; ν(CO) 1667; ν(CN) + ν(C=C) 1611. ^1H NMR (400 MHz, CD_2Cl_2, 213 K): δ 0.18, 0.75, 1.02, 1.07, 1.18, 1.34, 1.47, 1.56 (m, 3 H each, $P(CH(CH_3)_2)_2$), 1.48, 1.52 (s, 15 H each, $C_5(CH_3)_5$), 1.91, 2.21, 2.63, 3.00 (m, 1 H each, $P(CH(CH_3)_2)_2$), 3.62, 3.83 (s, 3 H each, $COOCH_3$), 5.51 (d, J_{HP} = 4.1 Hz, 1 H, NH), 5.65 (d, J_{HP} = 4.6 Hz, 1 H, NH), 5.94 (d, J_{HP} = 9.7 Hz, 1 H, HC≡C), 6.36 (s, 1 H, HC≡C), 6.32, 6.38, 6.66, 6.79, 6.93, 7.36, 7.44, 8.18, 8.24 (1 H each, C_5H_4N). $^{31}P\{^1H\}$ NMR (161.89 MHz, CD_2Cl_2, 213 K): δ 127.1, 129.9 (s). $^{13}C\{^1H\}$ NMR (100.57 MHz, CD_2Cl_2, 213 K): δ 8.7, 9.1 (s, $C_5(CH_3)_5$), 14.9, 16.4, 16.8, 17.5, 17.7, 17.9, 18.0, 18.2 (s, $P(CH(CH_3)_2)_2$), 28.7 (d, $^1J_{CP}$ = 20.1 Hz, $P(CH(CH_3)_2)$), 29.8 (d, $^1J_{CP}$ = 27.7 Hz, $P(CH(CH_3)_2)$), 30.2 (d, $^1J_{CP}$ = 12.5 Hz, $P(CH(CH_3)_2)$), 30.8 (d, $^1J_{CP}$ = 31.5 Hz, $P(CH(CH_3)_2)$), 52.6, 53.1 (s, $COOCH_3$), 74.4 (d, J_{CP} = 3.8 Hz, HC≡C), 77.1 (d, J_{CP} = 7.6 Hz, HC≡C), 80.9 (d, J_{CP} = 8.8 Hz, HC≡C), 100.3 (d, J_{CP} = 5 Hz, HC≡C), 98.5, 98.6 (s, $C_5(CH_3)_5$), 103.4, 109.3, 116.5, 117.5, 139.5, 139.9, 153.4, 154.0, 160.6, 160.8 (C_5H_4N), 161.0, 162.7 (s, CO). Data for **3b**: Yield 0.40 g, 68%. Anal. Calcd for $C_{54}H_{59}N_2BF_3PRu$: C, 69.3; H, 6.35; N, 3.0. Found: C, 69.2; H, 6.36; N, 2.8. IR (Nujol, cm^{-1}): ν(NH) 3247; ν(C≡C) 1816; ν(CN) + ν(C=C) 1605. ^1H NMR (400 MHz, CD_3COCD_3, 213 K): δ 0.12, 0.91, 0.99, 1.18, 1.19, 1.27, 1.32, 1.55 (m, 3 H each, $P(CH(CH_3)_2)_2$), 1.59, 1.68 (s, 15 H each, $C_5(CH_3)_5$), 1.54, 2.65, 2.75, 3.41 (m, 1 H each, $P(CH(CH_3)_2)_2$), 6.17 (s, 1 H, HC≡C), 6.36 (d, J_{HP} = 8.2 Hz, 1 H, HC≡C), 6.41, 6.89, 6.93, 7.04, 7.38, 7.58, 7.74, 8.66 (1 H each, C_5H_4N), 7.41, 6.90, 7.86, 7.82 (d, $^3J_{HH}$ = 8.6 Hz, 2 H each, $C_6H_4CF_3$), 8.00 (d, J_{HP} = 4.3 Hz, 1 H, NH), 8.13 (d, J_{HP} = 3.9 Hz, 1 H, NH). $^{31}P\{^1H\}$ NMR (161.89 MHz, CD_3COCD_3, 213 K): δ 124.2, 127.5 (s). $^{13}C\{^1H\}$ NMR (100.57 MHz, CD_3COCD_3, 213 K): δ 10.1, 10.5 (s, $C_5(CH_3)_5$), 17.2 (d), 17.4 (d), 17.8 (d), 19.3 (s), 19.4 (s), 19.5 (d), 19.7 (s), 19.9 (d) ($P(CH(CH_3)_2)_2$), 19.6 (d, $^1J_{CP}$ = 32.1 Hz, $P(CH(CH_3)_2)$), 29.3 (d, $^1J_{CP}$ = 29.5 Hz, $P(CH(CH_3)_2)$), 32.7 (d, $^1J_{CP}$ = 31.2 Hz, $P(CH(CH_3)_2)$), 34.0 (d, $^1J_{CP}$ = 14.3 Hz, $P(CH(CH_3)_2)$), 72.3 (d, J_{CP} = 6.8 Hz, HC≡C), 76.8 (s br, HC≡C), 85.2 (d, J_{CP} = 8.4 Hz, HC≡C), 86.5 (s br, HC≡C), 98.1 (s, $C_5(CH_3)_5$), 110.3, 110.6, 118.3, 118.8, 140.0, 140.9, 155.5, 156.2, 163.3, 163.7 (C_5H_4N), 126.6, 127.2, 130.2, 134.3 (s, $C_6H_4CF_3$), 128.7, 130.2 (q, $^1J_{CF}$ = 32.1 Hz, $C_6H_4CF_3$). ^{19}F NMR (376.26 MHz, CD_3COCD_3, 213 K): δ −62.9, −63.0 (s).

Kinetic Study of Alkyne to Vinylidene Isomerization. Samples of **1** in CD_3OD or CD_2Cl_2 containing a 10:1 molar excess of the corresponding alkyne HC≡CR (R = COOMe, $C_6H_4CF_3$) were immersed into a liquid N_2/ethanol bath to "freeze" the isomerization process during transport and handling. It was not possible to study the reaction of **1** with HC≡CCOOMe due to the occurrence of a highly exothermic cyclotrimerization catalytic reaction, which caused the solvent to boil (**CAUTION:** one NMR tube shattered due to the sharp difference in temperature between the reaction mixture and the cooling bath). The sample was removed from the bath and inserted into the probe of the NMR spectrometer at 273 K. Once shims were adjusted, the probe was warmed to the desired temperature. The NMR temperature controller was previously calibrated against a methanol sample, the reproducibility being ±0.5 °C. $^{31}P\{^1H\}$ NMR spectra were recorded for at least 2 half-lives at regular intervals using the spectrometer software for accurate time control. Peak intensities were

dx.doi.org/10.1021/ic401119p | Inorg. Chem. 2013, 52, 8919−8932

analyzed from stacked plots of the $^{31}P\{^{1}H\}$ NMR spectra. First-order rate constants were derived from the least-squares best-fit lines of the ln(intensity) versus time plots. The uncertainty in the isomerization rate constants represents one standard deviation ($\pm\sigma$) derived from the slope of the best-fit line. Uncertainties in the activation enthalpies and entropies were calculated from the uncertainties in the slope and intercept of the best-fit lines of the Eyring plots. Adaptations of the same protocol were followed for other kinetics measurements carried out in the present work.

Computational Details. All calculations were performed at the DFT level using the PBE0 functional[44] as implemented in Gaussian 09.[45] It has been shown that this functional performs well for second-row transition-metal complexes.[46] Additionally, some calculations were performed by means of the M06 functional[47] including an ultrafine integration grid.[48] The Ru atom was described using the scalar-relativistic Stuttgart-Dresden SDD pseudopotential[49] and its associated double-ζ basis set complemented with a set of *f*-polarization functions.[50] The 6-31G** basis set was used for the H,[51] C, N, O, F, P, and Cl atoms.[52] Diffuse functions were added for O, F, and Cl atoms[53] in all calculations. In order to achieve a proper description of the ion pairs, the structures of the reactants, intermediates, transition states, and products were fully optimized in methanol solvent (ε = 32.61) using the SMD continuum model.[54] Transition states were identified by having one imaginary frequency in the Hessian matrix. It was confirmed that transition states connect with the corresponding intermediates by means of application of the eigenvector corresponding to the imaginary frequency and subsequent optimization of the resulting structures. All energies collected in the text are Gibbs energies in methanol at 298 K. The chemical shielding tensors were computed using the GIAO method[55] as implemented in Gaussian 09[45] by means of the PBE0 functional.[44] NMR calculations were carried out using the IGLOO-III basis set for the H, C, N, O, F, Si, P, and Cl atoms[56] and the above-described SDD pseudopotential for the Ru atom. Proton chemical shifts were calculated as $\delta = \sigma(SiMe_4) - \sigma(complex)$, where σ stands for the isotropic chemical shielding of H. The geometry of the tetramethylsilane reference was optimized at the same level of theory as the studied complexes (6-31G**).

■ ASSOCIATED CONTENT

Supporting Information

Tables of rate constants for alkyne to vinylidene isomerization at different temperatures, in different solvents, and as a function of chloride concentration, calculated mechanism for isomer **II**, details of the pK_a computation, Cartesian coordinates and absolute energies, and Gibbs energies in methanol (Hartrees) of all calculated species. This material is available free of charge via the Internet at http://pubs.acs.org.

■ AUTHOR INFORMATION

Corresponding Author

*E-mail: manuel.tenorio@uca.es, carmen.puerta@uca.es, agusti@klingon.uab.es.

Notes

The authors declare no competing financial interest.

■ ACKNOWLEDGMENTS

We thank the Spanish "Ministerio de Economía y Competitividad" (DGICYT, Projects CTQ2010-15390, CTQ2011-23336, and ORFEO Consolider-Ingenio 2010 CSD2007-00006) and Junta de Andalucía (PAI FQM188, P08 FQM 03538) for financial support and Johnson Matthey plc for generous loans of ruthenium trichloride. M.A.O. also thanks the Spanish MECD for a FPU research grant. We are also grateful to CESCA for generous allocation of computer time.

■ REFERENCES

(1) (a) Höhn, A.; Werner, H. *J. Organomet. Chem.* **1990**, *382*, 255–272. (b) Rappert, T.; Nürnberg, O.; Mahr, N.; Wolf, J.; Werner, H. *Organometallics* **1992**, *11*, 4156–4164.

(2) (a) Bullock, R. M. *J. Chem. Soc., Chem. Commun.* **1989**, 165–167. (b) Lomprey, J. R.; Selegue, J. P. *J. Am. Chem. Soc.* **1992**, *114*, 5518–5523.

(3) de los Ríos, I.; Jiménez-Tenorio, M.; Puerta, M. C.; Valerga, P. *J. Am. Chem. Soc.* **1997**, *119*, 6529–6538.

(4) Puerta, M. C.; Valerga, P. *Coord. Chem. Rev.* **1999**, *193–195*, 977–1025.

(5) García-Yebra, C.; López-Mardomingo, C.; Fajardo, M.; Antiñolo, A.; Otero, A.; Rodríguez, A.; Vallat, A.; Luca, D.; Mugnier, Y.; Carbó, J. J.; Lledós, A.; Bo, C. *Organometallics* **2000**, *19*, 1749–1765.

(6) Bustelo, E.; Carbó, J.; Lledós, A.; Mereiter, K.; Puerta, M. C.; Valerga, P. *J. Am. Chem. Soc.* **2003**, *125*, 3311–3321.

(7) (a) Wakatsuki, Y. *J. Organomet. Chem.* **2004**, *684*, 4092–4109. (b) Tokunaga, M.; Suzuki, T.; Koga, N.; Fukushima, T.; Horiuchi, A.; Wakatsuki, Y. *J. Am. Chem. Soc.* **2001**, *123*, 11917–11924. (c) Wakatsuki, Y.; Koga, N.; Werner, H.; Morokuma, K. *J. Am. Chem. Soc.* **1997**, *119*, 360–366. (d) Wakatsuki, Y.; Koga, N.; Yamazaki, H.; Morokuma, K. *J. Am. Chem. Soc.* **1994**, *116*, 8105–8111.

(8) De Angelis, F.; Sgamellotti, A.; Re, N. *Organometallics* **2002**, *21*, 2715–2723.

(9) De Angelis, F.; Sgamellotti, A.; Re, N. *Organometallics* **2002**, *21*, 5944–5950.

(10) De Angelis, F.; Sgamellotti, A.; Re, N. *Dalton Trans.* **2004**, 3225–3230.

(11) De Angelis, F.; Sgamellotti, A.; Re, N. *Organometallics* **2007**, *26*, 5285–5288.

(12) Bianchini, C.; Peruzzini, M.; Vacca, A.; Zanobini, F. *Organometallics* **1991**, *10*, 3697–3707.

(13) Grotjahn, D. B.; Zeng, X.; Cooksy, A. L. *J. Am. Chem. Soc.* **2006**, *128*, 2798–2799.

(14) Grotjahn, D. B.; Zeng, X.; Cooksy, A. L.; Kassel, W. S.; DiPasquale, A. G.; Zakharov, L. N.; Rheingold, A. L. *Organometallics* **2007**, *26*, 3385–3402.

(15) Suresh, C. H.; Koga, N. *J. Theor. Comput. Chem.* **2005**, *4*, 59–73.

(16) Vastine, B. A.; Hall, M. B. *Organometallics* **2008**, *27*, 4325–4333.

(17) Cowley, M. J.; Lynam, J. M.; Slattery, J. M. *Dalton Trans.* **2008**, 4552–4554.

(18) Katayama, K.; Ozawa, H. *Coord. Chem. Rev.* **2004**, *248*, 1703–1715.

(19) Bruneau, C.; Dixneuf, P. H. *Angew. Chem., Int. Ed.* **2006**, *45*, 2176–2203.

(20) Grotjahn, D. B. *Chem.—Eur. J.* **2005**, *11*, 7147–7153.

(21) Grotjahn, D. B. *Dalton Trans.* **2008**, 6497–6508.

(22) (a) Singh, V. K.; Bustelo, E.; de los Ríos, I.; Macías-Arce, I.; Puerta, M. C.; Valerga, P.; Ortuño, M. A.; Ujaque, G.; Lledós, A. *Organometallics* **2011**, *30*, 4014–4031. (b) de los Ríos, I.; Bustelo, E.; Puerta, M. C.; Valerga, P. *Organometallics* **2010**, *29*, 1740–1749. (c) Otsuka, M.; Tsuchida, N.; Ikeda, Y.; Kimura, Y.; Mutoh, Y.; Ishii, Y.; Takano, K. *J. Am. Chem. Soc.* **2012**, *134*, 17746–17756.

(23) (a) Bustelo, E.; Jiménez-Tenorio, M.; Puerta, M. C.; Valerga, P. *Eur. J. Inorg. Chem.* **2001**, 2391–2398. (b) Aneetha, H.; Jiménez-Tenorio, M.; Puerta, M. C.; Valerga, P.; Mereiter, K. *Organometallics* **2003**, *22*, 2001–2013.

(24) Creati, F.; Coletti, C.; Re, N. *Organometallics* **2009**, *28*, 6603–6616.

(25) (a) Macchioni, A. *Chem. Rev.* **2005**, *105*, 2039–2073. (b) Clot, E. *Eur. J. Inorg. Chem.* **2009**, 2319–2328.

(26) Basallote, M. G.; Besora, M.; Castillo, C. E.; Fernández-Trujillo, M. J.; Lledós, A.; Maseras, F.; Máñez, M. A. *J. Am. Chem. Soc.* **2007**, *129*, 6608–6618.

(27) Kovács, G.; Ujaque, G.; Lledós, A. *J. Am. Chem. Soc.* **2008**, *130*, 853–864.

(28) (a) Appelhans, L. N.; Zuccaccia, D.; Kovacevic, D.; Chianese, A. R.; Miecznikowski, J. R.; Macchioni, A.; Clot, E.; Eisenstein, O.; Crabtree, R. H. *J. Am. Chem. Soc.* **2005**, *127*, 16299–16311. (b) Xia,

Y.; Dubnik, A. S.; Gevorgyan, V.; Li, Y. *J. Am. Chem. Soc.* **2008**, *130*, 6940−6941. (c) Boutadla, Y.; Davies, D. L.; Macgregor, S. A.; Poblador-Bahamonde, A. I. *Dalton Trans.* **2009**, 5820−5831.
(29) Macías-Arce, I.; Puerta, M. C.; Valerga, P. *Eur. J. Inorg. Chem.* **2010**, 1767−1776.
(30) Hydrogen bonding has been found to affect significantly the course of alkyne to vinylidene rearrangements at ruthenium centers bearing hemilabile phosphine ligands Grotjahn, D. B.; Miranda-Soto, V.; Kragulj, E. J.; Lev, D. A.; Erdogan, G.; Zeng, X.; Cooksy, A. L. *J. Am. Chem. Soc.* **2008**, *130*, 20−21.
(31) Díez, J.; Gimeno, J.; Merino, I.; Rubio, E.; Suárez, F. J. *Inorg. Chem.* **2011**, *50*, 4868−4881.
(32) Hyder, I.; Jiménez-Tenorio, M.; Puerta, M. C.; Valerga, P. *Organometallics* **2011**, *30*, 726−737.
(33) Kotha, S.; Brahmachary, E.; Lahiri, K. *Eur. J. Inorg. Chem.* **2005**, 4741−4767.
(34) Concerning phosphine dissociation processes in [Cp*Ru] species, late transition states involve low activation barriers with respect to the corresponding unsaturated ruthenium complexes Bryndza, H. E.; Domaille, P. J.; Paciello, R. A.; Bercaw, J. E. *Organometallics* **1989**, *8*, 379−385.
(35) Transition state **II-TS-4a-5a-Cl** is found 0.3 kcal mol^{-1} above the η^2-(C−H) intermediate **II-4a-Cl** in the energy profile in methanol, but it lies 1.5 kcal mol^{-1} below when the entropic correction for the solute is included (Gibbs energy profile).
(36) Intermediate **I-4a-Cl** does exist in the gas phase, and it is almost isoenergetic with respect to the hydrido−alkynyl species. A test calculation in methanol was also carried out using the M06 functional, but the η^2-(C−H) structure could not be found.
(37) Regarding the isomeric system **II**, the analogous transition state **II-TS-5a-2a-Cl** directly connects the hydride and the vinylidene complexes (see Supporting Information).
(38) Johnson, D. G.; Lynam, J. M.; Slattery, J. M.; Welby, C. E. *Dalton Trans.* **2010**, *39*, 10432−10441.
(39) Vyacheslav, S.; Bryantsev, V. S.; Diallo, M. S.; Goddard, W. A., III *J. Phys. Chem. B* **2008**, *112*, 9709−9719.
(40) (a) Kovács, G.; Rossin, A.; Gonsalvi, L.; Lledós, A.; Peruzzini, M. *Organometallics* **2010**, *29*, 5121−5131. (b) Díez, J.; Gimeno, J.; Lledós, A.; Suárez, F. J.; Vicent, C. *ACS Catal.* **2012**, *2*, 2087−2099.
(41) Our results are in good agreement with the previously computed pK_a^{THF} of 1.4 for the hydrido ligand in the related complex [Cp(PMe$_3$)$_2$Ru(H)C≡CC≡CH] (see ref 21).
(42) (a) Paton, R. S.; Maseras, F. *Org. Lett.* **2009**, *11*, 2237−2240. (b) Zhang, J.; Shen, W.; Li, L.; Li, M. *Organometallics* **2009**, *28*, 3129−3139. (c) Kovács, G.; Lledós, A.; Ujaque, G. *Organometallics* **2010**, *29*, 3252−3260. (d) Kovács, G.; Lledós, A.; Ujaque, G. *Organometallics* **2010**, *29*, 5919−5926. (e) Ariafard, A.; Asadollah, E.; Ostadebrahim, M.; Rajabi, N. A.; Yates, B. F. *J. Am. Chem. Soc.* **2012**, *134*, 16882−16890.
(43) Steinmetz, B.; Schenk, W. A. *Organometallics* **1999**, *18*, 943−946.
(44) (a) Perdew, J. P.; Burke, K.; Ernzerhof, M. *Phys. Rev. Lett.* **1996**, *77*, 3865−3868. (b) Perdew, J. P.; Ernzerhof, M.; Burke, K. *J. Chem. Phys.* **1996**, *105*, 9982−9985.
(45) Frisch, M. J.; Trucks, G. W.; Schlegel, H. B.; Scuseria, G. E.; Robb, M. A.; Cheeseman, J. R.; Scalmani, G.; Barone, V.; Mennucci, B.; Petersson, G. A.; Nakatsuji, H.; Caricato, M.; Li, X.; Hratchian, H. P.; Izmaylov, A. F.; Bloino, J.; Zheng, G.; Sonnenberg, J. L.; Hada, M.; Ehara, M.; Toyota, K.; Fukuda, R.; Hasegawa, J.; Ishida, M.; Nakajima, T.; Honda, Y.; Kitao, O.; Nakai, H.; Vreven, T.; Montgomery, J. A.; , Jr., Peralta, J. E.; Ogliaro, F.; Bearpark, M.; Heyd, J. J.; Brothers, E.; Kudin, K. N.; Staroverov, V. N.; Kobayashi, R.; Normand, J.; Raghavachari, K.; Rendell, A.; Burant, J. C.; Iyengar, S. S.; Tomasi, J.; Cossi, M.; Rega, N.; Millam, J. M.; Klene, M.; Knox, J. E.; Cross, J. B.; Bakken, V.; Adamo, C.; Jaramillo, J.; Gomperts, R.; Stratmann, R. E.; Yazyev, O.; Austin, A. J.; Cammi, R.; Pomelli, C.; Ochterski, J. W.; Martin, R. L.; Morokuma, K.; Zakrzewski, V. G.; Voth, G. A.; Salvador, P.; Dannenberg, J. J.; Dapprich, S.; Daniels, A. D.; Ö. Farkas, Foresman, J. B.; Ortiz, J. V.; Cioslowski, J.; Fox, D. J. *Gaussian 09*, Revision A.1; Gaussian, Inc.: Wallingford, CT, 2009.
(46) (a) Quintal, M. M.; Karton, A.; Iron, M. A.; Boese, A. D.; Martin, J. M. L. *J. Phys. Chem. A* **2006**, *110*, 709−716. (b) Waller, M. P.; Braun, H.; Hojdis, N.; Bühl, M. *J. Chem. Theory Comput.* **2007**, *3*, 2234−2242.
(47) Zhao, Y.; Truhlar, D. G. *Theor. Chem. Acc.* **2008**, *120*, 215−241.
(48) Wheeler, S. E.; Houk, K. N. *J. Chem. Theory Comput.* **2010**, *6*, 395−404.
(49) Andrae, D.; Haeussermann, U.; Dolg, M.; Stoll, H.; Preuss, H. *Theor. Chim. Acta* **1990**, *77*, 123−141.
(50) Ehlers, A. W.; Bohme, M.; Dapprich, S.; Gobbi, A.; Hollwarth, A.; Jonas, V.; Kohler, K. F.; Stegmann, R.; Veldkamp, A.; Frenking, G. *Chem. Phys. Lett.* **1993**, *208*, 111−114.
(51) Hehre, W. J.; Ditchfield, R.; Pople, J. A. *J. Chem. Phys.* **1972**, *56*, 2257−2261.
(52) Francl, M. M.; Pietro, W. J.; Hehre, W. J.; Binkley, J. S.; Gordon, M. S.; DeFrees, D. J.; Pople, J. A. *J. Chem. Phys.* **1982**, *77*, 3654−3665.
(53) Clark, T.; Chandrasekhar, J.; Spitznagel, G. W.; Schleyer, P. *J. Comput. Chem.* **1983**, *4*, 294−301.
(54) Marenich, A. V.; Cramer, C. J.; Truhlar, D. G. *J. Phys. Chem. B* **2009**, *113*, 6378−6396.
(55) (a) London, F. *J. Phys. Radium* **1937**, *8*, 397−409. (b) McWeeny, R. *Phys. Rev.* **1962**, *126*, 1028−1034. (c) Ditchfield, R. *Mol. Phys.* **1974**, *27*, 789−807. (d) Wolinski, K.; Hilton, J. F.; Pulay, P. *J. Am. Chem. Soc.* **1990**, *112*, 8251−8260. (e) Cheeseman, J. R.; Trucks, G. W.; Keith, T. A.; Frisch, M. J. *J. Chem. Phys.* **1996**, *104*, 5497−5509.
(56) Kutzelnigg. W.; Fleischer, U.; Schindler, M. *The IGLO-Method: Ab Initio Calculation and Interpretation of NMR Chemical Shifts and Magnetic Susceptibilities*; Springer-Verlag: Heidelberg, 1990; Vol. *23*.